Contributions of throughfall, forest and soil characteristics to near-surface soil water-content variability at the plot scale in a mountainous Mediterranean area

Molina, A.J.[1*], Llorens, P.[1], Garcia-Estringana, P.[2], Moreno de las Heras, M. [1], Cayuela, C.[1], Gallart, F. [1], Latron, J. [1]

[1]Surface Hydrology and Erosion Group, Institute of Environmental Assessment and Water Research (IDAEA), CSIC, Barcelona, Spain.

[2] Instituto Madrileño de Investigación y Desarrollo Rural, Agrario y Alimentario (IMIDRA), Madrid, Spain.

*Corresponding author:

Institute of Environmental Assessment and Water Research (IDAEA), CSIC, Jordi Girona 18-26, 08034 Barcelona, Spain

antonio.molina@idaea.csic.es

Tel.: +34 93 400 61 00

Abstract

Soil water-content (SWC) variability in forest ecosystems is affected by complex interactions between climate, topography, forest structure and soil factors. However, detailed studies taking into account the combined effects of these factors are scarce. This study's main aims were to examine the control that throughfall exerts on local spatial variation of near-surface soil water-content and to combine this information with forest structure and soil characteristics, in order to analyze all their effects together. Two stands located in the Vallcebre Research Catchments (NE Spain) were studied: one dominated by *Quercus pubescens* and the other by *Pinus sylvestris*. Throughfall and the related shallow SWC were monitored in each plot in 20 selected locations. The main characteristics of the nearest tree and soil parameters were also measured. The results indicated that mean SWC increment at the rainfall event scale showed a strong linear relationship with mean throughfall amount in both forest plots. The % of locations with SWC increments increased in a similar way to throughfall amount in both forest plots. The analyses considering all the effects together indicated again that throughfall had a significant positive effect in both forest plots, while soil litter depth showed a significant negative effect for the oak plot but lower statistical significance for the pine plot, showing a comparable –although more erratic– influence of the organic forest floor for this plot. These results, together with lower responses of SWC to throughfall than expected in rainfall events characterized by low preceding soil water-condition and high rainfall intensity, suggest that litter layer is playing an important role in controlling the soil water-content dynamics. The biometric characteristics of the nearest trees showed significant but very weak relationships with soil water-content increment, suggesting that stemflow and throughfall may act at lower distances from tree trunk than those presented in our study.

Keywords: rainfall partitioning, soil moisture, soil water repellence, forest hydrology

1. Introduction and Objectives

Spatio-temporal variations in surface water fluxes in forests are better understood than variations in the unsaturated zone. The greater number of factors involved in unsaturated zone dynamics, along with the non-linearity of several of the driving mechanisms controlling this dynamic, have led, in the last decade, to significantly more field and modelling studies, focusing on near-surface soil moisture patterns at different spatio-temporal scales (e.g. Romano et al., 2011; Guswa and Spencer, 2012; Garcia-Estringana et al., 2013; Baroni et al., 2013; Molina et al., 2014; Hu et al., 2018).

In addition to meteorological, topographic and soil factors, vegetation factors have a great influence on near-surface soil water-content variability (Tromp-van Meerveld and McDonnell, 2006). Different degrees of influence of these driving factors lead to different degrees of data structuring (Nielsen et al., 1973; Koster and Suarez, 2001), although a white noise pattern, probably due to inappropriate scale approximation, can also be detected (Blöschl and Sivapalan, 1995). Grayson et al. (1997) proposed two types of factors controlling soil water-content spatial variability at the catchment scale, whose effects depend on the relationship between precipitation and evapotranspiration: non-local controls, present when lateral soil water movements are dominant (precipitation>evapotranspiration), and local controls, when the vertical water movements of soil infiltration, drainage and evapotranspiration dominate the spatial patterns (precipitation<evapotranspiration). In Mediterranean areas, subsurface water redistribution is limited to short periods of time, while the vertical fluxes that are not connected to upslope contributing areas depend greatly on vegetation and soil distribution within the catchment (Gomez-Plaza et al., 2001). Consequently, the control of vegetation on rainfall partitioned into throughfall (diffuse water input) and stemflow (point water input), transpiration and soil properties such as soil organic content or soil structure play a fundamental role in soil water-content spatial variation at the plot scale (Tromp-van Meerveld and McDonnell, 2006; Brocca et al., 2007; Liang et al., 2011; Beven and Germann, 2013).

Studies of soil water-content at the plot scale can be classified according to the approach followed and the subsequent objectives. On the one hand, several studies have focused mainly on characterizing spatial and/or temporal variability *per se*. The approaches followed in these studies aim 1) to relate spatial variation of soil water-content, through the coefficient of variation or standard deviation, to mean soil water conditions (Hupet and Vanclooster, 2002; Brocca et al., 2007; Molina et al., 2014); 2) to study temporal persistence of soil water-content patterns through temporal stability or Spearman rank correlation analyses (Vachaud et al., 1985; Comegna and Basile, 1994; Molina et al., 2014); and 3) to study spatial aggregation or data structuring of soil water-content by geostatistics (Wendroth et al., 1999; Brocca et al., 2007). On the other hand, some studies have focused on incorporating soil physics into hydrological modelling by means of pedotransfer functions, which correlate hydrodynamic soil behavior with more easily measurable soil properties (Saxton et al., 1986; De Vos et al., 2005). Between these two contrasting approaches, a wide variety of field studies have focused on the expected driving factors of local soil water-content variation. The factors analyzed normally correspond to one of the "compartments" (climate, vegetation, soil), with little information about the others and any possible interactions. Liang et al. (2011) studied the influence of stemflow and root-induced bypass flow on soil water dynamics around trees on a hillslope. Schume et al. (2003) explained soil water-content's spatio-temporal variability in a mixed forest through geostatistical tools and complementary measurements of tree positions. Gallardo (2003) observed that spatial variation in both soil properties and soil water-content was clearly related to the distance to flooding source (edge of the pond) in a floodplain forest. Raat et al. (2002) compared the spatial patterns of throughfall with those of surface soil water-content in a Douglas forest stand through temporal stability analyses. Finally, Bialkowski and Buttle (2015) carried out a detailed study at the tree scale in which soil water monitoring was complemented with measurements of soil parameters and tree structure. All these studies point out that further integration of information from climate, vegetation and soil factors is still needed for a better understanding of local soil water-content variability.

In the Vallcebre research area (south Pyrenees), field observations and data modelling have been carried out for more than three decades in order to improve the understanding of hydrological processes at catchment and plot scales in mountainous Mediterranean areas where forests play a critical role (Llorens et al., 2018). Rainfall partitioned into throughfall, stemflow and soil water-content has been measured separately in forest plots within the area (Llorens et al., 1997; Mużyło et al., 2012; Garcia-Estringana et al., 2013; Cayuela et al., 2018). The main aim of this study is to analyze the control that rainfall partitioned into throughfall exerts on the local spatial variation of near-surface soil water-content within the two most representative forest ecosystems in the area. Therefore, we combined throughfall information with characteristics of the forest structure and soils to reveal their interacting effects and how they vary within and between the study plots at the rainfall event scale.

2. Materials and Methods

2.1. Site description and experimental set-up

The monitored areas lie within the Cal Rodó catchment (4.17 km^2, altitude from 1,104 to 1,643 m a.s.l) in the Vallcebre research area. The Vallcebre research area (Latron et al., 2010a; Llorens et al., 2018) is located on the southern edge of the Pyrenees at the headwaters of the Llobregat River. The area is close to Vallcebre village, 130 km north-east of Barcelona, NE Spain (42 º12´12´´N, 1 º49´3´´E). The research area was selected in early 1990 to analyze the hydrological consequences of land abandonment, as well as the hydrological and sediment yield behavior of badlands areas. Before and during the 19th century, hill-slopes were deforested and terraces, 10–20 m wide, were built for agricultural use over more than 35% of the catchment area (Poyatos et al., 2003). During the second half of the 20th century, these terraces were steadily abandoned as a consequence of the migration of rural population to urban areas. Then, spontaneous afforestation by *Pinus sylvestris* L. resulted in a general increase of forest cover from 1.6% in 1967 to 17.8% in 1996 (Poyatos et al., 2003). In the non-terraced areas, small forest patches of *Quercus pubescens* Willd. are present, as the climax vegetation in the zone. Climate is defined as humid Mediterranean and is highly seasonal, leading to periods with a high water deficit in summer (Latron et al., 2010b); mean annual temperature at 1,260 m a.s.l. is 9.1ºC and long-term (1983–2006) mean ± standard deviation of annual precipitation is 862 ± 206 mm, with an average of 90 rainy days per year. The rainiest seasons are autumn and spring, while in summer convective storms also provide significant precipitation input. Long-term mean ± standard deviation (1989–2006) of annual potential evapotranspiration, calculated by the Hargreaves and Samani method (Hargreaves and Samani, 1985), is 823 ± 26 mm.

Two experimental plots were established (1 km apart) to study the spatial variation of throughfall and soil water-content in the representative forested areas within the catchment (Figure 1). The monitoring period extended from 1 May 2013 to 31 October 2013. One plot was placed in a forest patch dominated by oaks (42 º12´14´´N, 1 º49´20´´E) and dense understory in a non-terraced area, while the other was established in an old terraced area covered by overgrown pines with scarce understory (42 º11´43´´N, 1 º49´13´´E) (Cayuela et al., 2018). The oak plot has an area of 2,200 m^2 and its mean slope is close to 0º (Rubio, 2005). The main overstory species is *Quercus pubescens;* other woody species are *Prunus avium* and *Fraxinus excelsior*. The understory is mainly composed of *Buxus sempervirens, Prunus spinosa* and *Rosa spp.*, while the herbaceous stratum covers nearly 65% of the soil surface (Poyatos et al., 2005). Soil has a silty-clay-loam texture and is about 50 cm deep (Rubio, 2005). The pine plot has an area of 900 m^2 and is formed by two flat terraces descending to the NNE with a general slope close to 15º. The vegetation consists of an overstory of *Pinus sylvestris* and there is low presence of understory vegetation, mainly represented by isolated *Prunus spinosa* individuals. The herbaceous stratum covers nearly 90% of the soil surface. Soil has a silty-loam texture and soil depth is normally greater than 1 m. Forest structure of the studied plots is shown in Table 1.

Before the experimental measurements and during a period when oaks had foliage, 50 hemispherical photographs were randomly taken in each forest plot with a fisheye objective (180º 1:2.8D EX 15-mm SIGMA lens) mounted on a Nikon D300S camera, mounted on a tripod. The images were used to describe the spatial variability of forest cover and provide criteria for selecting 20 locations to place the devices for monitoring throughfall and soil water-content in each forest plot. The canopy cover was obtained for each hemispherical photograph by taking a radius equivalent to a zenith angle of 8.9º, as detailed in Llorens and Gallart (2000), through the Gap Light Analyzing software (Frazer et al., 1999). Ten forest-cover classes of different lengths, each with 5 photographs, were defined. To choose 2 locations per class, random numbers between 1 and 1000 were generated, and the 2 smallest numbers of each class generated were selected, resulting in 20 locations selected per plot. Figure 1 shows a map of the forest plots with the positions of the throughfall tipping buckets and TDR probes.

2.2. Field measurements

2.2.1. Bulk rainfall and throughfall

Bulk rainfall was measured for both forest plots by automatic standard rain gauges (AW-P, Institut Analitic, 0.2 mm resolution) located in nearby clearings at 1 m height, while throughfall was measured, also at 1 m height, by automatic standard rain gauge (Davis Rain Collector II, Davis, 0.2 mm resolution). All the resulting data were recorded every 5 minutes by dataloggers (DT80 Datataker, Thermo Fisher Scientific Inc.). Square sections of rigid plastic were placed below each throughfall gauge to ensure that the throughfall water collected by the gauges was splashed after measurement and no artificial preferential flows of water reaching the soil were caused (Figure 1). Rain gauges were cleaned and the gauges were re-calibrated every 1-2 months by static calibration (Calder and Kidd, 1978).

2.2.2. Soil water-content

In each forest plot, soil water-content (SWC, cm^3 cm^{-3}) was monitored every 20 minutes with twenty 30 cm-long TDR probes (CS605 probes, Campbell Scientific) installed at an angle of 30º to the surface, thus monitoring the first 20 cm of soil depth. TDR probes were controlled by SMDX50 multiplexers (Campbell Scientific) and a TDR100 (Campbell Scientific) connected to a data logger (CR10X, Campbell Scientific).

Since TDR measurements performed with a Tektronix 1502-C cable tester (Tektronix communications) in the soils of the study area correlate well with measurements derived from gravimetric samples (Rabadà, 1995), the installed probes were connected to the Tektronix 1502-C cable tester for manual measurement every 20-30 days. SWC was then calculated for both types of measurements by the Topp equation (Topp et al., 1980) and compared, resulting in a linear calibration equation for each forest plot (R^2 of 0.60 and 0.96 for the oak and the pine plots, respectively).

Finally, the Savitzky-Golay smoothing filter (package “signal”, R Core Team, 2013), which preserves peak heights and widths of the original signal, was applied to reduce the noise in the time series of the calibrated SWC.

2.2.3. Soil characteristics

By the end of the study period, soil characteristics were obtained in 9 locations per plot systematically selected according to their average SWC values during the study period. For each plot, the averages were first ranked and split into 3 classes (low, intermediate and high SWC). For each SWC class, three locations were randomly selected. In total, 18 cubic holes of approximately 20x20x20 cm were excavated for soil determinations.

The thickness of the first layer of forest floor consisting of fresh leaves on the surface (litter; L or A_{00}) was measured and averaged from the 4 faces of each excavated hole. The resulting fractions of litter and soil taken from the holes were placed in a portable fridge for laboratory determinations; and the hole volumes were determined, to calculate soil bulk density. The particle density of mineral soil material was assumed to be 2.65 g/cm^3, and then soil porosity (%) was calculated from particle density and soil bulk density.

Particle sizes of the mineral soil fraction were analyzed by combining sieves and a laser diffraction particle size analyser (Malvern Mastersizer/E) with previous laboratory treatments for removing organic matter content and dispersing clay aggregates in soil samples. Soil texture was determined by the USDA texture classification. In addition, organic and inorganic carbon fractions of the soil matrix (SOC and SIC, respectively) were obtained by ignition, following the recommendations and the corrections proposed in Wang et al. (2012).

2.2.4. Architecture of the nearest trees

Canopy cover information was complemented by determinations of several biometric characteristics of the nearest trees to each pair of throughfall and SWC measurement locations. Diameter at breast height (DBH) was determined by means of a forest tape, and total tree height, height of the first branch and branch angles were calculated by a hypsometer (Haglöf vertex IV); and branch diameters, by a caliper with laser pointers (Haglöf Mantax Black with Gator eyes). The tree crown was considered as an ellipse and projected radii were used to calculate crown area and volume.

2.3. Data analysis

2.3.1. Soil and forest structure

T-student's tests were used to test for differences in the soil and forest structure variables between the forest plots (p-value<0.05). Previously, data were examined for normality and homogeneity of variance by the Kolmogorov and the Levene tests, respectively.

2.3.2. Rainfall and throughfall

Rainfall events were defined according to the time needed for the canopy to dry between two successive rains, taking 6 and 12 hours for day- and night-times, respectively (Llorens et al., 2014). In total, 34 rainfall events above 1 mm rainfall amount were considered for further analysis along the 6 months of the study period. The main rainfall and throughfall characteristics (amount, mean and maximum intensity in 5 minutes and duration), together with the environmental conditions during rainfall, were calculated for each rainfall event analyzed. The non-parametric Kruskall-Wallis test based on the chi-squared statistic was used to test for differences in the main rainfall and throughfall characteristics between the forest plots (p-value<0.05) due to lack of normality or homoscedasticity.

2.3.3. *Soil water-content*

The SWC data series and the derived SWC increments were analyzed for each rainfall event and probe. The increments were calculated as the differences between the measurements 2 hours before the beginning of rainfall and the maximum SWC during rainfall. SWC measurements were extended to the end of 2013, in order to find a week of measurements with no rainfall and very low evapotranspirative demand, in which the maximum difference observed between two successive 20-minute measurements was taken as the systematic error for that TDR probe. Thus, when SWC increment was equal to or lower than this systematic error, a non-response was considered for that probe.

2.3.4. *Temporal stability of throughfall and soil water-content*

Temporal stability (Vachaud et al., 1985) was calculated (i) to identify whether positions of high or low throughfall persisted between rainfall events, i.e. to find locations with throughfall either consistently higher or lower than the mean value over all the study period; and (ii) to compare throughfall patterns with those for SWC. The procedure described by Raat et al. (2002) was followed, in which a normalized measure of throughfall and soil water-content for each rainfall event is calculated as ($\hat{X}_i$):

$$\hat{X}_i = \frac{(X_i - \bar{X})}{\bar{X}}$$

where X_i are throughfall/soil water-content values at one location *i* and $\bar{X}$ is the mean rainfall-event value from all the locations in that rainfall event. With the plotting of the means over time of the normalized values (n=20) ranked from smallest to largest, this parametric method of assessing relative data differences permits a graphic representation of temporal stability between locations.

2.3.5. *Relationship of soil water-content with independent factors: general linear mixed models*

To test for the effect of independent factors in explaining the local spatio-temporal variation in SWC during the rainfall events within each forest plot, general linear mixed models (GLMMs; Crawley, 2013) with repeat-measurement structure were fitted to data from locations where soils were sampled (n=9 for each plot). The dependent variable was the increment in the SWC for each event and location, while the independent variables (fixed factors and covariates) were: those characterizing throughfall (such as maximum throughfall intensity or throughfall amount), soil (such as SOC or soil density) and forest/tree structure (such as forest cover or DBH of the nearest tree) (variables in Tables 2 and 3). Site was applied as a random factor accounting for the variability in repeated measurements over time. Rainfall event was also defined as a crossed random factor to control for event-scale dependence of individual throughfall measurements.

Collinearity pre-screening for the model predictor variables was assessed using bivariate Pearson's R correlations. Where two predictors significantly correlated between them, we excluded for GLMM analysis the covariate/factor that showed the lowest correlation score with the observed SWC increments. In order to find the most parsimonious model configuration, alternative GLMMs were thus compared for different combinations of pre-screened independent variables according to the Akaike Information Criterion (AIC; Akaike, 1973). AIC is a model optimality measure that trades off complexity and the fit of the model. The selected, optimal GLMM structure was tested for statistical significance of the included factors and covariates. Standardized β coefficients and goodness of fit were also determined for the optimal model structure. Goodness of fit was assessed using both the conditional and marginal coefficients of determination, following the approach described by Nakagawa and Schielzeth (2013) for mixed-effect models. Conditional R^2 accounts for the proportion of variance explained by the fixed predictors and the random (site and event) factors. Differently, marginal R^2 provides an estimation for the proportion of variance explained exclusively by the fixed predictors. All data analyses were carried out using the R software (R Core Team, 2013).

3. Results

3.1. Soil and forest structure characteristics

Soil properties and biometric characteristics of the nearest tree for each pair of throughfall and SWC measurements are shown in Tables 2 and 3, respectively. T-student's tests revealed that litter and SIC were significantly higher in the pine plot. Soil particle distribution also differed between the forest plots, with silty-clay texture for the oak plot and silty-loam for the pine plot.

The main significant differences in tree biometrics were observed in total tree height and vertical distance to the first alive branch. Both were much higher in the pines as a common consequence of high light competition in this type of high-density stand formed by spontaneous afforestation.

3.2. General patterns of rainfall, throughfall and soil water-content

The 34 rainfall events under analysis accounted for 333 and 347 mm in the oak and pine plots, respectively. Non-significant differences were observed in the non-parametric

Kruskall-Wallis tests when comparing rainfall characteristics between the forest plots (n= 34, p-values of 0.873, 0.864, 0.624 and 0.844 for rainfall amount, duration, mean intensity and maximum intensity, respectively). The rainfall amount ranged from 1.1 to 39.5 mm; 32% of the events were higher than 10 mm and 15% were higher than 20 mm. The mean and maximum rainfall intensities were 3.8 ± 5.2 and 22.0 ± 23.3 mmh^{-1} (means ± standard deviations), while rainfall duration ranged from 0.2 to 37.5 hours. A detailed description of the rainfall characteristics and the meteorological conditions during the rainfall events is shown in Appendix A.

The mean cumulative throughfall during the study period was 270.7 ± 30.7 mm and 257.0 ± 38.5 mm for the oak and pine plots, respectively. The highest differences observed in the cumulative throughfall between collectors were 113.9 mm for the oak plot and 187.9 mm for the pine plot. The mean relative throughfall at the event scale (expressed as % of bulk rainfall) ranged from 17 to 92% (mean, median and interquartile range of 70, 75 and 55-86%, respectively) and from 5 to 90% (mean, median and interquartile range of 57, 63 and 37-77%, respectively), while the means ± standard deviations of the mean and the maximum values for throughfall intensity were 3.0 ± 5.3 and 19.8 ± 23.7 mmh^{-1} and 2.7 ± 4.1 and 17.0 ± 21.1 mmh^{-1} for the oak and pine plots, respectively. Kruskal-Wallis tests indicated that mean throughfall and both mean and maximum intensities did not significantly differ between the plots (n= 34, p-values of 0.598, 0.835 and 0.358, respectively). As expected, mean relative throughfall increased with bulk rainfall and throughfall variability, expressed by the coefficient of variation (CV, %), which was stabilized at approximately 20% over 10 mm of rainfall (Figure 2). However, throughfall spatial variability behaved differently between the plots, as observed in throughfall dispersion and indicated by the variation in the Fisher skewness coefficient for the rainfall events. The oak plot showed a relatively high number of dripping locations (relative throughfall higher than 100%), especially for rainfall amounts smaller than 10 mm, whereas the pine plot showed throughfall distributions more skewed to the left (skewness<0) in most of the rainfall events (Figure 2). Finally, throughfall showed no significant relationship with the variables measured in the nearest trees. Nor were significant differences on throughfall observed when grouping the tipping buckets by tree characteristics and comparing mean throughfall values. In contrast, both plots showed a significant pattern of decreasing throughfall as mean canopy cover increased in the 60% to 100% range (Figure 3).

The median time series of SWC from the 20 locations highlight the differences between the forest plots in temporal and spatial variabilities (Figure 4). The maximum SWC, and the SWC observed after 2 days without rain preceded by saturated soil conditions as a proxy for field capacity, were both higher in the oak plot (means of 0.54 and 0.42 cm^{3}cm^{-3}) than in the pine plot (means of 0.40 and 0.31 cm^{3}cm^{-3}), while the minimum SWC was very similar in the two plots (0.18 *versus* 0.19 cm^{3}cm^{-3}). This indicated that the mineral soil horizon in the oak plot had a greater maximum capacity for retaining water after saturation. On the other hand, the differences between the maximum SWC values and soil porosity in the plots (values are showed in Table 2) could be explained by the fact that SWC probes were inserted without taking out the litter horizon, representing up to 50% of soil volume for some locations in the pine plot. SWC spatial variability was also higher in the oak plot, as indicated by a difference of about 50% in the interquartile ranges.

3.3. The single effect of throughfall on soil water-content variability

The inter- and intra-rainfall event variability in SWC was clearly affected by throughfall amount and intensity, as expected. However, rainfall events 16 and 25 for the oak plot and only the latter for the pine plot showed a much lower SWC response to throughfall than the other events. These outliers, collected in summer, showed low previous SWC conditions, high rainfall amounts (19.2 to 39.2 mm) and the highest rainfall intensities (62.7 to 114.6 $mm \cdot h^{-1}$) (more details of rainfall characteristics are shown in Appendix A).

For intra-rainfall event variability, 6 rainfall events with high rainfall (>19 mm) and contrasting prior SWC conditions (0.25 to 0.45 $cm^3 \cdot cm^{-3}$ and 0.21 to 0.34 $cm^3 \cdot cm^{-3}$ for the oak and pine plots, respectively) were selected to show the relationships between throughfall and soil water-content dynamics at this fine temporal scale (Figure 5 and Appendix B).

Throughfall variability during rainfall, expressed by the standard deviation, was clearly related to throughfall intensity, with the greatest differences between throughfall values observed during high bursts of throughfall. The responses of mean SWC to throughfall amount during rainfall were greater in all the selected rainfall events except for those considered outliers. In addition, SWC variability decreased with increased SWC in most of the rainfall events and showed the opposite trend for the outliers, with variability increasing once throughfall started to reach the soil surface.

Regarding inter-rainfall event variability, the mean values of SWC increments correlated significantly with those for throughfall, while mean SWC during rainfall did not (Figure 6). The frequency of locations showing responses to throughfall (see 2.3.3 section for details about calculations of SWC increment) was clearly affected by throughfall amount in both plots: a positive linear response was observed up to 10 mm of throughfall (or up to 15 mm of rainfall), followed by a plateau in which most of the locations showed SWC increases

(Figure 7). The correlations between SWC and throughfall amount improved significantly when the outliers were excluded, as expected from the intra-rainfall variability analyses. Finally, the temporal stability (TS) analyses gave contrasting results for the forest plots. When the TS values for throughfall were compared with those for mean SWC and SWC increments, no statistically significant correlations were observed in the pine plot. On the contrary, in the oak plot, linear relationships were significant for both SWC series and were better for SWC increments (Figure 8). According to the better correlations between SWC increments and throughfall amount, SWC increments were considered for further analyses.

3.4. The combined effects of throughfall, forest and soil characteristics affecting soil water-content variability

Collinearity pre-screening showed that several throughfall and forest structure variables strongly correlated between them (Appendix C in the supplementary material). In accordance with the obtained Pearson's R scores, throughfall amount (TF), forest cover (FC) and crown volume of the nearest tree (V), soil bulk density, (ps), litter thickness (Ao) and soil organic carbon content (SOC) were retained for GLMM analysis of the local variations of SWC increment. The GLMM configuration that resulted in the most parsimonious structure takes throughfall amount and litter thickness as model predictor covariates best explaining the local increments in SWC (Appendix D in the supplementary material). Interestingly, increasing GLMM complexity with the incorporation of other predictors did no translate into significant increases in the variance explained by the model. For the oak plot, conditional R^2 of the model was 93%, with the standardized β coefficients indicating significant positive and negative effects for throughfall amount and litter thickness, respectively (Table 4). For the pine plot, conditional R^2 was 94% and only throughfall amount significantly affected SWC increments. The marginal R^2 values, as those that account for the proportion of variance explained exclusively by the fixed (TF and Ao) model predictors, were 38% and 46% for the oak and pine plot, respectively.

4. Discussion

Previous research at the experimental site of Vallcebre have separately studied rainfall partitioning and soil water dynamics in forested areas (Llorens et al., 1997; Mużyło et al., 2012; Garcia-Estringana et al., 2013; Cayuela et al., 2018). The main aim of this study was to analyze the control that throughfall exerts on the local spatial variation of near-surface soil water-content within the two most representative forest ecosystems in the area.

The general characteristics of the rainfall partitioned into throughfall were very similar between the two forest plots (non-significant differences observed in the statistical comparisons of the main characteristics), accounting for a small difference of 13 mm in the accumulated value for the entire study period. The mean cumulated throughfall values in this study (81% of bulk rainfall for oaks during the leafed period and 74.7% for pines) are equivalent to those found previously in the study area (Llorens et al., 1997; Muzylo et al., 2012). The decreasing linear pattern of throughfall in canopy cover ranging from 60 to 100% (Figure 3) was similar in the forest plots, with a loss of significance below 60%. This result showing throughfall reduction when forest cover increases is in line with other studies relating rainfall interception increase to canopy cover (e.g., Teklehaimanot et al., 1991; Jackson, 2000; Deguchi et al., 2006; Molina and Del Campo, 2012). In contrast, non-significant relationships were found between throughfall and all the variables measured in the nearest trees (Table 3). The similarity in the mean cumulated values of throughfall and in the relationship with canopy cover between the forest plots (Figure 3) contrasted with the differences in spatial throughfall patterns observed at rainfall event scale (Figure 2). While the oak plot had a relatively high number of locations with high throughfall concentration (i.e. dripping points), especially for rainfall amounts smaller than 10 mm, the pine plot had several locations with the opposite trend (i.e. locations with very low throughfall), especially for rainfall amount higher than 10 mm, where most of rainfall events showed left skewed distribution. Thus, although our data at event scale may suggest that spatial throughfall variability is site-dependent and somehow related to local forest properties (Levia et al., 2011), this local dependency seems to disappear at higher temporal aggregation. As also observed by Holwerda et al. (2006), spatial differences tend to be counterbalanced at longer time steps, as indicated by our similar relationships between cumulative throughfall and canopy cover in the forest plots. However, the loss of a significant canopy cover effect on throughfall from 60% downward in both plots remains unclear.

For soil water-content, we first studied the single effect of throughfall on intra- and inter-rainfall event variability, to further analyze how throughfall, soil and forest characteristics affected soil water-content responses during the rainfall events studied through GLMMs. Both intra- and inter-rainfall event analyses indicated that throughfall plays an important role controlling the spatial and temporal variations of SWC (Figures 5, 6 and 7). The relationship between mean SWC increment and bulk rainfall amount was highly significant for both the oak and pine plots. However, within-rainfall event mean SWC was not significantly linked to water input (Figure 6). Mean SWC during the rainfall was calculated for the time span elapsed from the beginning of the rainfall event to 6/12 hours (for day/night) after the last tipping bucket pulse was recorded, therefore integrating part of the SWC recession curve. The influence of the recession dynamics in this variable is, to a large extent, responsible for the loss of significant relationship with the rainfall input. This effect was particularly important where quick soil water drainage was taking place during the recession dynamics.

The temporal stability analyses provide a way to study the consistency between the spatial patterns of throughfall and SWC (Vachaud et al., 1985; Raat et al., 2002). The temporal stability of SWC, both SWC means and increments, was weakly related to that of throughfall in the oak plot, but did not show any clear relationships for the pine plot (Figure 8). This suggests that spatial consistency over time in SWC can be only partially explained by that in throughfall in the oak plot. Using SWC increments to compare the temporal stability between throughfall and soil water-content from the uppermost soil layer in a forest stand in The Netherlands, Raat et al. (2002) found no significant relationship between their patterns. The authors argued that the spatial pattern in SWC was not only affected by the pattern in throughfall amount but also by those in litter thickness and soil drainage. Other works have compared the spatial variation of SWC with that in forest structure as an indirect way to characterize rainfall partitioning dynamics. Schume et al. (2003) observed that the spatial organization of SWC under mature trees from two species behaved differently due to their contrasting tree architecture. These authors, however, also pointed out that the erratic SWC behavior observed during intense showers with dry antecedent soil water conditions may be explained by a dynamic macropore system led by a marked shrinking of clay aggregates during drying out period, but also by the entrapping of air in the outermost soil layer. Similarly, Bialkowski and Buttle (2015) showed that throughfall and stemflow significantly contributed to SWC recharge in a maple sugar tree but not for pine trees of different ages, given their differences in tree architecture. Our temporal stability results support that tree architecture was somehow affecting the spatial throughfall patterns just for the oak plot, although no significant correlations between characteristics of the nearest trees and throughfall were observed (Appendix C in the supplementary material).

Over 10 mm of throughfall, most of the locations showed significant SWC increments in both plots (Figure 7). This result is consistent with common finding of rainfall interception studies, which normally consider 8 mm of rainfall (as short and intense showers) as the minimum amount required for saturating the canopy cover (Klaasen et al., 1998; Molina and Del Campo, 2012). According to our results, saturation capacity is reached shortly before 10 mm of throughfall for mature stands of *Pinus sylvestris* and *Quercus pubescens*, when SWC increase is observed in most locations below the canopy. However, special attention should be paid to two high-intensity rainfall events (>20 mm) collected in summer with fewer locations responding to throughfall than other rainfall events (from 75 to 90% of the total locations) with similar rainfall amount (Figure 7), which worsened the relationship between SWC increment and throughfall (Figure 6). One hypothesis for this is that soil water repellence could have played a more active role in the SWC dynamics than other factors (e.g., macropore structure) for these two events, which were characterized by dry antecedent soil conditions and high rainfall intensity. In a broad review on this topic, Doerr et al. (2000) indicated that it is commonly accepted that soil water repellence in forest ecosystems is caused by organic compounds derived from living or decomposing plants and microorganisms, as well as by the root activity of plants with resins or aromatic oils, such as eucalyptus and pines. Doerr and Thomas (2000) tried to understand whether there was a threshold in soil water-content for sandy loam and loamy sand soils, in which the soil behaved as either water-repellent or non-repellent. The authors pointed out that repellence was absent when soil moisture exceeded 28%, but they also showed that, after wetting, repellence was not necessarily re-established when soils became dry again. In another study focusing on the effects of forest floor characteristics in the hydrodynamic behavior of Andisols in the Canary Islands, Neris et al. (2013) observed that water repellence had a significant effect in reducing infiltration capacity and promoting runoff in both pine and rainforest plots, although it was greater for the former, where the wetting front remained mostly on the forest floor and barely penetrated into the soil mineral part. They attributed this effect mainly to the duff layer's characteristics (i.e. cohesion and hydrophobicity), which may vary considerably with litter characteristics. In our case, although we did not directly measure duff layer properties, our very high SOC values (75% of locations showed SOC values about 4% in both plots) may be indicative of great organic decomposition and mineralization processes taking place at transient soil layers that may probably affected water infiltration. Another alternative hypothesis explaining the lower SWC increments for these two events may be the entrapping of air in the outermost soil layers, which can reduce importantly the infiltration capacity of the soils (Schume et al., 2003).

Our GLMM results (Table 4) highlighted a positive influence of throughfall amount on the dynamics of soil water content, indicating a strong control of surface soil moisture by spatially distributed effective rainfall inputs. Differently, the surface litter layer of the plots showed a negative influence for the observed dynamics, reducing the increments of soil water content during the events under increased litter thickness. These conflicting effects were partially expected: litter thickness enhances soil surface porosity (as calculated in this work) but this effect is not necessarily translated into higher soil water holding capacity given the low capacity of this material to retain water (Luna et al., 2017). In our case, maximum SWC values (Figure 4) never reached the determined soil porosity for the studied oak and pine forest floor materials (around 60%, Table 2), thus suggesting a low capacity for retaining water in both types of litter. Given the very extensive surface organic layer developed in the pine plot (in some locations up to 50% of the explored surface soil volume was occupied by litter) we expected a more pronounced negative effect of litter thickness on the observed SWC increments for the pine floor. The obtained standardized β coefficients for the effect of litter layer control on the analyzed per-event surface soil-water increments showed, however, a similar magnitude (near -0.20) but lower statistical significance for the pine plot, suggesting a comparable –although more erratic– influence of the organic forest floor. Overall these results highlight the complex dynamics that rule the vertical and horizontal water movements at the interface between the litter and the mineral part of soils (Schume et al, 2003; Lin and Shoe, 2008; Beven and Germann, 2013).

Finally, Pearson correlations between the biometric variables and the SWC increments (Appendix C in the supplementary material) showed, in a few cases (e.g., forest cover), significant but very weak (Pearson's R $\leq$0.1) relationships. Liang et al. (2011) found a significant influence of stemflow water redistribution on SWC dynamics close to tree trunk. Cayuela et al. (2018), when studying stemflow rates in trees in the same forest plots as in the present study, observed a marked variability in the lag time between the beginning of rainfall and the beginning of stemflow, ranging from 0 to 6 hours. The differences in the operating times between throughfall and stemflow and in the activation of different soil infiltration pathways (Liang et al., 2011) make our experimental design unsuitable for studying the combined effects of these two water inputs on the SWC variability. Therefore, the distances from tree trunk in which stemflow and throughfall can be differently affecting SWC dynamics remain unclear for the studied species.

5. Conclusions

The results given in this study highlight how complex the local spatio-temporal variation of soil water-content is in mature forests of heterogeneous forest structure and developed organic layers. As expected, throughfall amount showed linear relationships with soil water-content responses. It also had a clear effect on the frequency of these responses, with most locations being activated with throughfall higher than 10 mm in both forest plots regardless of the previous soil water conditions. In contrast, the low magnitude and frequency observed in two rainfall events with greater precipitation and low previous soil water conditions led us to hypothesize that water repellence was playing a more active role in this departure from normality than those played by other factors such as the macropore network. The study of some soil properties has indicated that the litter layer played a significant role in SWC increments during rainfall in the oak plot, making locations with higher litter thickness less responsive to throughfall. In the pine plot, despite of the higher range and magnitude of litter thickness, its effect showed lower statistical significance, suggesting a comparable –although more erratic– influence of the organic forest floor. The biometric characteristics of the nearest trees showed very weak relationships with soil water increments, so stemflow may act at a lower distances and higher temporal scales than those presented in this study. According to our results, further research is recommended into the role of litter but also into the effects of stemflow and throughfall at lower distances from tree trunks in order to improve our understanding of dynamics on soil water response at the rainfall scale.

Acknowledgements

This research was supported by the projects TransHyMed (CGL2016-75957-R AEI/FEDER, UE) and MASCC-DYNAMITE (PCIN-2017-061/AEI) funded by the ‘‘Agencia Estatal de Investigación”. A.J. Molina and M. Moreno de las Heras are beneficiaries of Juan de la Cierva post-doctoral fellowships; and C. Cayuela, of an FPI grant, all of them funded by the Spanish Ministry of Economy and Competitiveness. Support provided by A. Löchner, X. Huguet, M. Roig-Planasdemunt, E. Sánchez-Costa, G. Bertran is also acknowledged. The constructive comments of two anonymous reviewers on an earlier version of this manuscript are thanked.

6. Bibliography

- Akaike, H. (1973). A new look at the statistical model identification. IEEE Transactions on Automatic Control, 19, 716-723
- Baroni, G., Ortuani, B., Facchi, A., Gandolfi, C. (2013). The role of vegetation and soil properties on the spatio-temporal variability of the surface soil moisture in a maize-cropped field. Journal of Hydrology, 489, 148-159.
- Beven, K., Germann, P. (2013). Macropores and water flow in soils revisited. Water Resources Research, 49, 3071-3092.
- Bialkowski, R., Buttle, J. M. (2015). Stemflow and throughfall contributions to soil water recharge under trees with differing branch architectures. Hydrological Processes, 29, 4068-4082.
- Blöschl, G., Sivapalan, M. (1995). Scale issues in hydrological modelling: a review. Hydrological processes, 9, 251-290.

- Brocca, L., Morbidelli, R., Melone, F., Moramarco, T. (2007). Soil moisture spatial variability in experimental areas of central Italy. Journal of Hydrology, 333, 356-373.
- Calder, I. R., Kidd, C. H. R. (1978). A note on the dynamic calibration of tipping-bucket gauges. Journal of hydrology, 39, 383-386.
- Cayuela, C., Llorens, P., Sanchez-Costa, E., Levia, D. F., Latron, J. (2018). Effect of biotic and abiotic factors on inter and intra-event variability in stemflow rates in oak and pine stands in a Mediterranean mountain area. Journal of Hydrology.
- Comegna, V., Basile, A. (1994). Temporal stability of spatial patterns of soil water storage in a cultivated Vesuvian soil. Geoderma, 62, 299-310.
- Crawley, M.J. (2013). Mixed-effects models. In: Crawley, M.J. (Ed.), The R Book, 2nd Ed. John Wiley and Sons Ltd., Chichester, pp. 681-784.
- Deguchi, A., Hattori, S., Park, H. T. (2006). The influence of seasonal changes in canopy structure on interception loss: application of the revised Gash model. Journal of Hydrology, 318, 80-102.
- De Vos, B., Van Meirvenne, M., Quataert, P., Deckers, J., Muys, B. (2005). Predictive quality of pedotransfer functions for estimating bulk density of forest soils. Soil Science Society of America Journal, 69, 500-510.
- Doerr, S. H., Thomas, A. D. (2000). The role of soil moisture in controlling water repellency: new evidence from forest soils in Portugal. Journal of Hydrology, 231, 134-147.
- Doerr, S. H., Shakesby, R. A., Walsh, R. (2000). Soil water repellency: its causes, characteristics and hydro-geomorphological significance. Earth-Science Reviews, 51, 33-65.

- Frazer, G. W., Canham, C. D., Lertzman, K. P. (1999). Gap Light Analyzer (GLA), Version 2.0: Imaging software to extract canopy structure and gap light transmission indices from true-colour fisheye photographs, user's manual and program documentation. Simon Fraser University, Burnaby, British Columbia, and the Institute of Ecosystem Studies, Millbrook, New York, 36.
- Gallardo, A. (2003). Spatial variability of soil properties in a floodplain forest in northwest Spain. Ecosystems, 6, 564-576.
- Garcia Estringana, P. (2011). Efectos de diferentes tipos de vegetación mediterránea sobre la hidrología y la pérdida de suelo. PhD Thesis. Universidad de Alcalá.
- Garcia-Estringana, P., Latron, J., Llorens, P., Gallart, F. (2013). Spatial and temporal dynamics of soil moisture in a Mediterranean mountain area (Vallcebre, NE Spain). Ecohydrology, 6, 741-753.
- Gómez-Plaza, A., Martınez-Mena, M., Albaladejo, J., Castillo, V. M. (2001). Factors regulating spatial distribution of soil water content in small semiarid catchments. Journal of hydrology, 253, 211-226.
- Grayson, R. B., Western, A. W., Chiew, F. H., Blöschl, G. (1997). Preferred states in spatial soil moisture patterns: Local and nonlocal controls. Water Resources Research, 33, 2897-2908.
- Guswa, A. J., Spence, C. M. (2012). Effect of throughfall variability on recharge: application to hemlock and deciduous forests in western Massachusetts. Ecohydrology, 5, 563-574.
- Hargreaves, G. H., Samani, Z. A. (1985). Reference crop evapotranspiration from temperature. Applied engineering in agriculture, 1, 96-99.

- Holwerda, F., Scatena, F. N., Bruijnzeel, L. A. (2006). Throughfall in a Puerto Rican lower montane rain forest: a comparison of sampling strategies. Journal of Hydrology, 327, 592-602.
- Hu, W., Liu, G., Zhang, X. (2018). A pore-scale model for simulating water flow in unsaturated soil. Microfluidics and Nanofluidics, 22, 71.
- Hupet, F., Vanclooster, M. (2002). Intraseasonal dynamics of soil moisture variability within a small agricultural maize cropped field. Journal of Hydrology, 261, 86-101.
- Jackson, N. A. (2000). Measured and modelled rainfall interception loss from an agroforestry system in Kenya. Agricultural and Forest Meteorology, 100(4), 323-336.
- Koster, R. D., Suarez, M. J., 2001. Soil moisture memory in climate models. *Journal* of hydrometeorology, 2, 558-570.
- Klaassen, W., Bosveld, F., De Water, E. (1998). Water storage and evaporation as constituents of rainfall interception. Journal of Hydrology, 212, 36-50.
- Latron, J, Llorens, P., Soler, M., Poyatos, R., Rubio, C., Muzylo, A., Martinez-Carreras, N., Delgado, J., Regües, D., Catari, G., Nord, G., Gallart, F. (2010a). Hydrology in a Mediterranean Mountain Environment – The Vallcebre Research Basins (Northeastern Spain). I. 20 years of Investigation of Hydrological Dynamics, vol. 336. IAHS-AISH Publication, pp. 38–43.
- Latron, J., Soler, M., Llorens, P., Nord, G., Gallart, F. (2010b). Hydrology in a Mediterranean Mountain Environment – The Vallcebre Research Basins (Northeastern Spain). II. Rainfall Runoff Relationships and Runoff Processes, vol. 336. IAHS-AISH Publication, pp. 151–156.

- Levia, D. F., Keim, R. F., Carlyle-Moses, D. E., Frost, E. E. (2011). Throughfall and stemflow in wooded ecosystems. In Forest Hydrology and Biogeochemistry (pp. 425-443). Springer Netherlands.
- Liang, W. L., Kosugi, K. I., Mizuyama, T. (2011). Soil water dynamics around a tree on a hillslope with or without rainwater supplied by stemflow. Water Resources Research, 47(2).
- Lin, H., Zhou, X. (2008). Evidence of subsurface preferential flow using soil hydrologic monitoring in the Shale Hills catchment. European Journal of Soil Science, 59, 34-49.
- Llasat, M. C. (2001). An objective classification of rainfall events on the basis of their convective features: application to rainfall intensity in the northeast of Spain. International Journal of Climatology, 21(11), 1385-1400.
- Llorens, P., Poch, R., Latron, J., Gallart, F. (1997). Rainfall interception by a Pinus sylvestris forest patch overgrown in a Mediterranean mountainous abandoned area I. Monitoring design and results down to the event scale. Journal of hydrology, 199, 331-345.
- Llorens, P., Gallart, F. (2000). A simplified method for forest water storage capacity measurement. Journal of Hydrology, 240, 131-144.
- Llorens, P., Domingo, F., Garcia-Estringana, P., Muzylo, A., Gallart, F. (2014). Canopy wetness patterns in a Mediterranean deciduous stand. Journal of hydrology, 512, 254-262.
- Llorens, P., Gallart, F., Cayuela, C., Roig-Planasdemunt, M., Casellas, E., Molina, A. J., Moreno de las Heras, M., Bertran, G., Sanchez-Costa, E., Latron, J. (2018). What have we learnt about Mediterranean catchment hydrology? 30 years observing

hydrological processes in the Vallcebre research catchments. Cuadernos de Investigación Geográfica.

- Luna, L., Miralles, I., Lázaro, R., Contreras, S., Solé-Benet, A. (2017). Effect of soil properties and hydrologic characteristics on plants in a restored calcareous quarry under a transitional arid to semiarid climate. Ecohydrology, e1896.
- Molina, A. J., del Campo, A. D. (2012). The effects of experimental thinning on throughfall and stemflow: a contribution towards hydrology-oriented silviculture in Aleppo pine plantations. Forest Ecology and Management, 269, 206-213.
- Molina, A. J., Latron, J., Rubio, C. M., Gallart, F., Llorens, P. (2014). Spatio-temporal variability of soil water content on the local scale in a Mediterranean mountain area (Vallcebre, North Eastern Spain). How different spatio-temporal scales reflect mean soil water content. Journal of hydrology, 516, 182-192.
- Mużyło, A., Llorens, P., Domingo, F. (2012). Rainfall partitioning in a deciduous forest plot in leafed and leafless periods. Ecohydrology, 5, 759-767.
- Nakagawa, S., Schielzeth, H. (2013). A general and simple method for obtaining R^2 from generalized linear mixed-effect models. Methods Ecol Evol, 4,133–42.
- Neris, J., Tejedor, M., Fuentes, J., Jimenez, C. (2013). Infiltration, runoff and soil loss in Andisols affected by forest fire (Canary Islands, Spain). Hydrological Processes, 27, 2814-2824.
- Nielsen, D. R. J. W., Biggar, J. W., Erh, K. T. (1973). Spatial variability of field-measured soil-water properties. Hilgardia, 42, 215-259.
- Poyatos, R., Latron, J., & Llorens, P. (2003). Land use and land cover change after agricultural abandonment: the case of a Mediterranean mountain area (Catalan Pre-Pyrenees). Mountain research and development, 23, 362-368.

- Poyatos, R., Llorens, P., Gallart, F. (2005). Transpiration of montane Pinus sylvestris L. and Quercus pubescens Willd. forest stands measured with sap flow sensors in NE Spain. Hydrology and Earth System Sciences Discussions, 2, 1011-1046.
- Raat, K. J., Draaijers, G. P. J., Schaap, M. G., Tietema, A., Verstraten, J. M. (2002). Spatial variability of throughfall water and chemistry and forest floor water content in a Douglas fir forest stand. Hydrology and Earth System Sciences Discussions, 6, 363-374.
- Rabadà, D. (1995). Dinàmica hidrològica d'una petita conca pirenaica de camps abandonats amb pinedes en expansió (Alt Berguedà, Barcelona). PhD Tesis, Institut de Ciències de la Terra ''Jaume Almera''(CSIC) i Dept. de Geoquímica, Petrologia i Prospecció Geològica. Rodríguez-Iturbe, I., Isham, V., Cox, D. R., Manfreda, S., Porporato, A. (2006). Space-time modeling of soil moisture: Stochastic rainfall forcing with heterogeneous vegetation. Water Resources Research, 42(6).
- Romano, N., Palladino, M., Chirico, G. B. (2011). Parameterization of a bucket model for soil-vegetation-atmosphere modeling under seasonal climatic regimes. Hydrology and Earth System Sciences, 15, 3877-3893.
- R Core Team. (2013). R: A language and environment for statistical computing. R Foundation for Statistical Computing, Vienna, Austria. ISBN 3-900051-07-0, URL http://www.R-project.org/.
- Rubio, C., 2005. Hidrodinámica de los suelos de un área de montaña media mediterránea sometida a cambios de uso y cubierta. PhD Tesis, Universitat Autònoma de Barcelona.

- Teklehaimanot, Z., Jarvis, P. G., Ledger, D. C. (1991). Rainfall interception and boundary layer conductance in relation to tree spacing. Journal of Hydrology, 123, 261-278.
- Topp, G., Davis, J., Annan, A.P., 1980. Electromagnetic determination of soil water content: measurements in coaxial transmission lines. Water Resour. Res. 16, 574–582.
- Tromp-van Meerveld, H. J., McDonnell, J. J. (2006). On the interrelations between topography, soil depth, soil moisture, transpiration rates and species distribution at the hillslope scale. Advances in Water Resources, 29, 293-310.
- Saxton, K. E., Rawls, W., Romberger, J. S., Papendick, R. I. (1986). Estimating generalized soil-water characteristics from texture 1. Soil Science Society of America Journal, 50, 1031-1036.
- Schume, H., Jost, G., Katzensteiner, K. (2003). Spatio-temporal analysis of the soil water content in a mixed Norway spruce (Picea abies (L.) Karst.)–European beech (Fagus sylvatica L.) stand. Geoderma, 112, 273-287.
- Vachaud, G., Passerat de Silans, A., Balabanis, P., Vauclin, M. (1985). Temporal stability of spatially measured soil water probability density function1. Soil Science Society of America Journal, 49, 822-828.
- Wang, X., Wang, J., Zhang, J. (2012). Comparisons of three methods for organic and inorganic carbon in calcareous soils of northwestern China. PlOS one, 7, e44334.
- Wendroth, O., Pohl, W., Koszinski, S., Rogasik, H., Ritsema, C. J., Nielsen, D. R. (1999). Spatio-temporal patterns and covariance structures of soil water status in two Northeast-German field sites. Journal of Hydrology, 215, 38-58.

Figure captions:

Figure 1. Maps of the forest plots with the positions of the throughfall tipping buckets and TDR probes. The picture on the left shows the monitor set up in the oak plot, whereas the pine plot is shown on the right (photos by J. Latron).

Figure 2. Relative throughfall (TH, % of bulk rainfall), coefficient of variation (CV, %) and Fisher skewness coefficient (skewness) *versus* bulk rainfall for the 20 monitored locations and the 34 rainfall events for each forest plot. Discontinuous lines indicate relative throughfall equal to100% of bulk rainfall and Fisher skewness coefficient equal to zero.

Figure 3. Cumulative throughfall (mm) during the study period *versus* canopy cover for the 20 monitored locations. Linear regressions were fitted for canopy cover greater than 60%. Note the presence of an outlier in the pine plot (right) with much lower cumulative throughfall than at the other locations.

Figure 4. Soil water-content dynamics (medians, 25 and 75% percentiles) in the forest plots (0-20 cm depth) during the study period.

Figure 5. Soil water-content and throughfall dynamics (means and standard deviations) in three selected rainfall events with rainfall higher than 19 mm.

Figure 6. Relationships between mean throughfall and mean SWC (top) and between mean throughfall and mean SWC increments (bottom) for the rainfall events studied (n=34 for each forest plot). Linear regressions were fitted when significant and without considering outliers (filled symbols) (see text for details).

Figure 7. Relationships between the frequency of SWC increments and the mean throughfall in the forest plots (n=34 rainfall events).

Figure 8. Ranking in the time stability plots (TS, means and standard deviations) for throughfall (a and d), SWC means and mean SWC increments (b and e). Relationships between time stability for throughfall, for SWC means and for mean SWC increments (c and f). Linear regressions were fitted when significant.

Appendix B: Soil water-content and throughfall dynamics (means and standard deviations) in three selected rainfall events with precipitation greater than 19 mm.

Table 1. Forest structure variables in the experimental plots. Different letters indicate significant differences in the mean values (standard deviations in brackets) between the forest plots (t-student test, $p<0.05$).

	Oak plot	Pine plot
Diameter at Breast Height (cm)	20.7 (8.2)a	19.9 (9.2)b
Tree Density (tree ha^{-1})	518	1189
Basal Area ($m^2 ha^{-1}$)	20.1	45.1
Height (m)	11.9 (3.2)a	17 (4.4)b
Canopy cover (%)	78.3 (18)a	69.3 (17.7)b

Table 2. Soil properties of the experimental plots (means and standard deviations). Different letters indicate significant differences in the mean values between the forest plots (t-student test, p-value<0.05).

	Oak plot	Pine plot
Thickness of litter (cm)	1.64 (0.73)a	4.72 (2.35)b
Dry weight of litter (g/cm^2)	98.40 (118.29)a	349.10 (195.93)b
Volumetric gravel content (%)	3.53 (2.80)a	2.87 (1.04)a
Sand (%)	9.70 (0.80)a	4.19 (2.73)b
Silt (%)	57.52 (4.17)a	71.90 (2.05)b
Clay (%)	32.80 (3.76)a	23.91 (0.68)b
Soil bulk density ($g\ cm^{-3}$)	1.03 (0.09)a	0.99 (0.21)a
Soil porosity (%)	61.10 (3.38)a	62.63 (7.93)a
SOC (%)	5.84 (1.98)a	5.88 (2.30)a
SIC (%)	0.77 (0.68)a	5.62 (1.78)b

Table 3. Biometric characteristics of the nearest trees (means and standard deviations). Different letters indicate significant differences in the mean values between the forest plots (t-student test, p-value<0.05).

	Oak plot	Pine plot
Distance to pair of devices (m)	2.14 (0.95)a	1.29 (0.42)b
DBH (cm)	22.52 (6.94)a	22.12 (9.63)a
Total tree height (m)	12.84 (2.57)a	17.36 (4.16)b
Height to first branch (m)	4.33 (2.42)a	10.53 (2.29)b
Crown area (m^2)	23.46 (18.66)a	13.76 (11.97)a
Crown volume (m^3)	274.40 (228.71)a	155.20 (178.19)a
Depth of bark (m)	0.99 (0.50)a	2.33 (1.19)b
Branch angle (º)	30.96 (19.23)a	24.14 (21.55)a

Table 4. Statistical results for the most optimum GMLM tested for every plot according to the AIC Information Criterion. Rainfall events considered outliers were discarded from analyses (n=288 for each forest plot). ***p-value<0.001, ** p-value<0.05, * p-value<0.1. Standard variations for the standardized β coefficients are showed in brackets.

	β coefficients		F		p-value	
Independent variables	Oak plot	Pine plot	Oak plot	Pine plot	Oak plot	Pine plot
Throughfall amount (TF, mm)	0.56 (0.06)***	0.66 (0.05)***	152.82	269.95	<0.0001	<0.0001
Litter thickness (Ao, cm)	-0.23 (0.09)**	-0.16 (0.11)	8.29	2.91	0.02	0.13

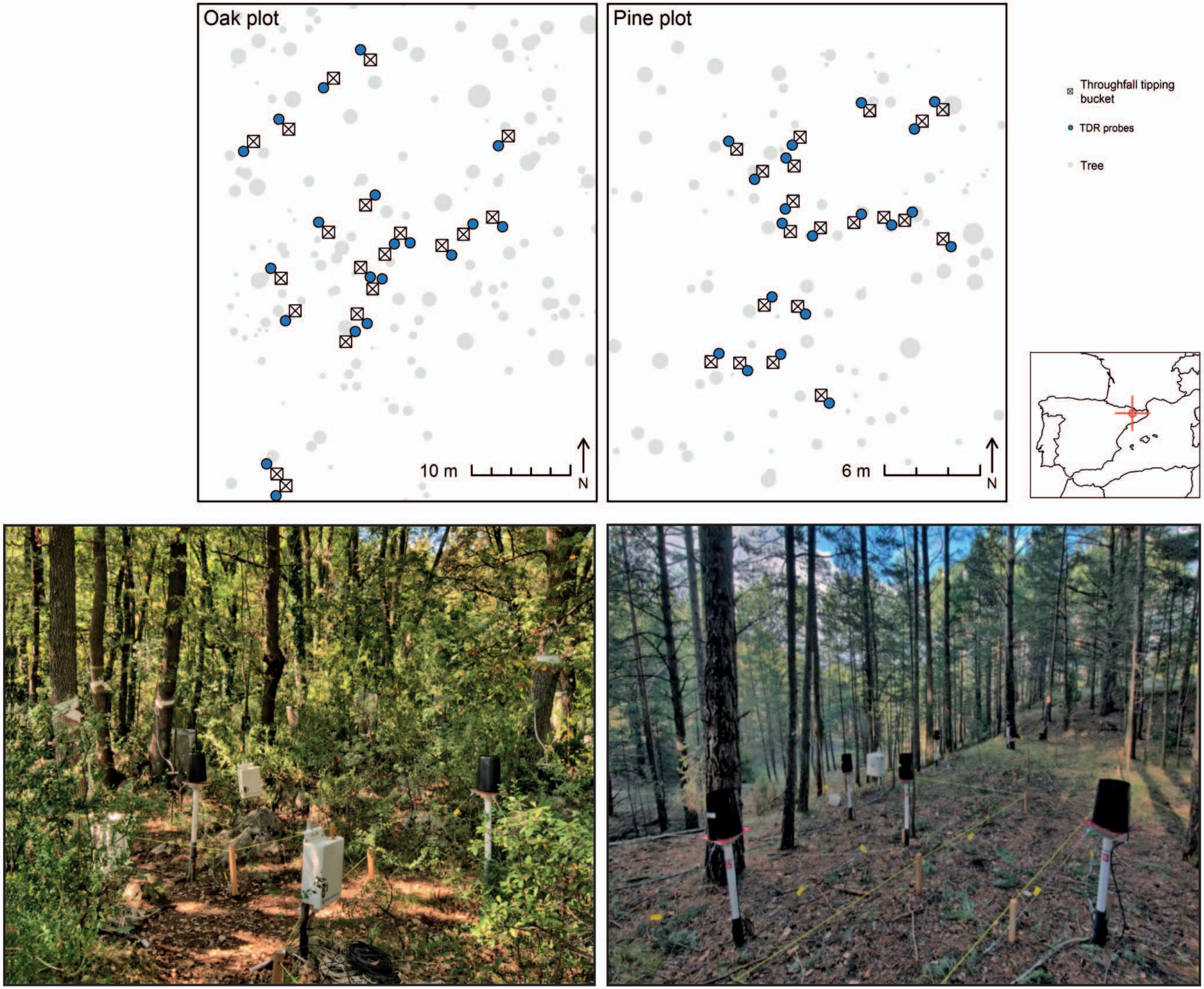
Oak plot
10 m
N
Pine plot
6 m
N
Throughfall tipping bucket
TDR probes
Tree

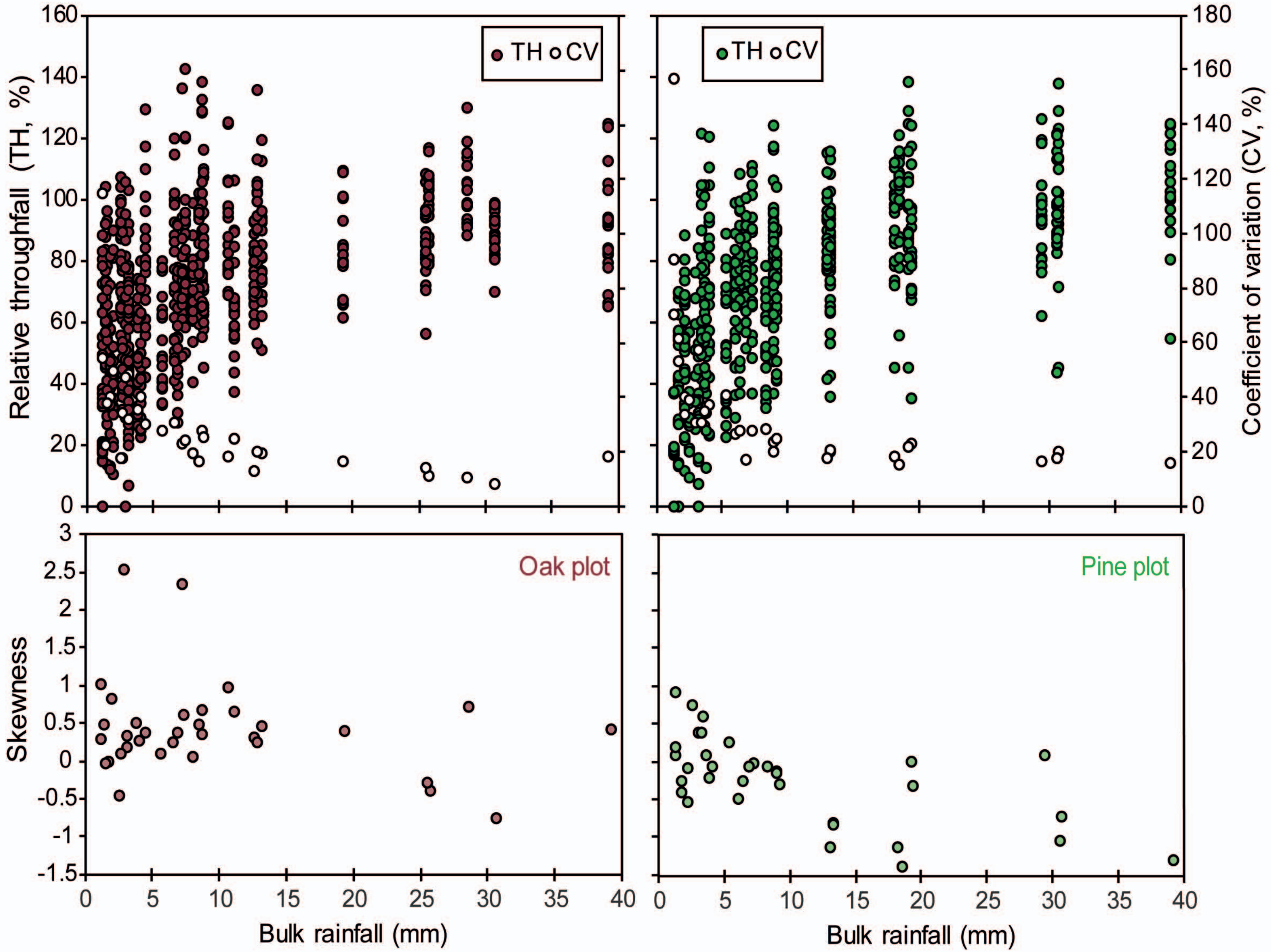

TH
CV
TH
CV
Oak plot
Pine plot
Relative throughfall (TH, %)
Coefficient of variation (CV, %)
Skewness
Bulk rainfall (mm)
Bulk rainfall (mm)

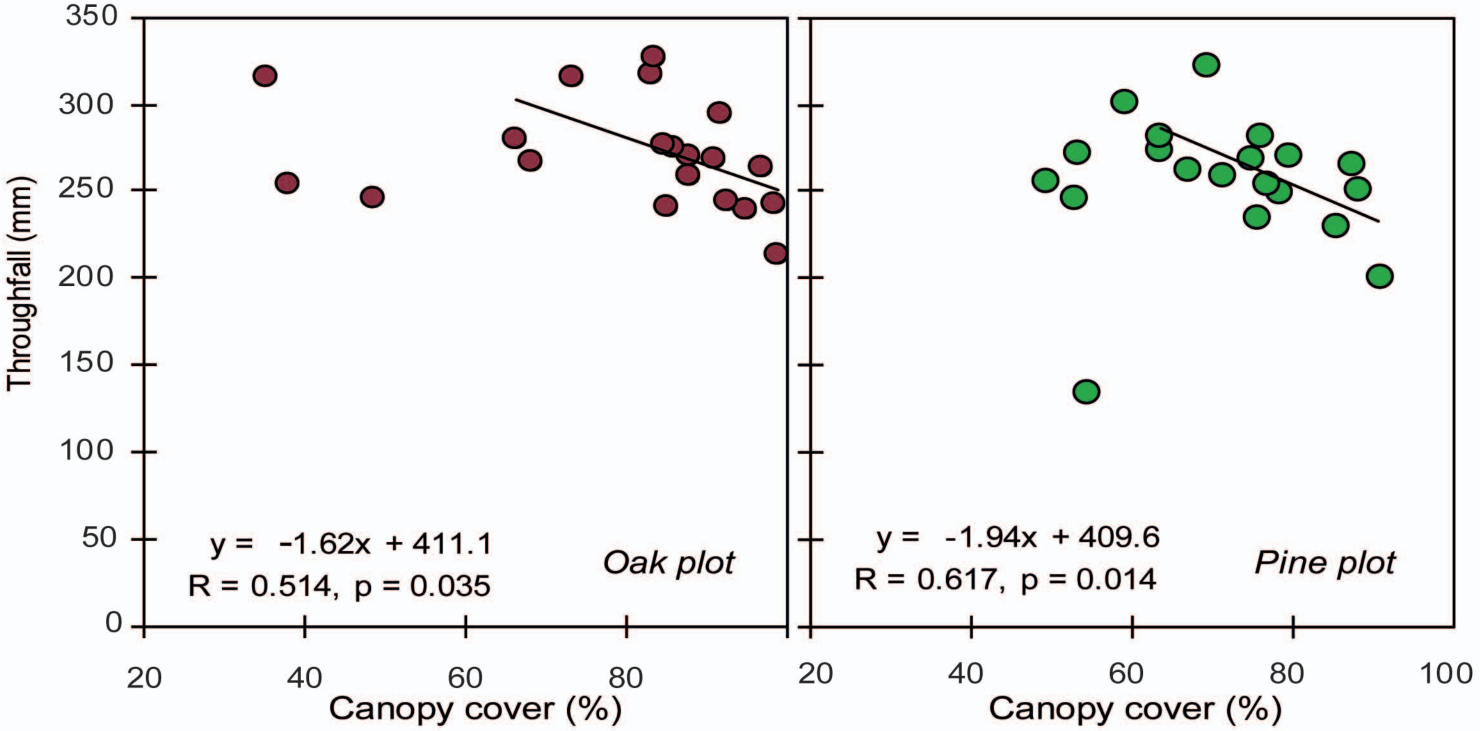

Throughfall (mm)
350
300
250
200
150
100
50
0
20
40
60
80
100
Canopy cover (%)
Canopy cover (%)
y = -1.62x + 411.1
R = 0.514, p = 0.035
Oak plot
y = -1.94x + 409.6
R = 0.617, p = 0.014
Pine plot

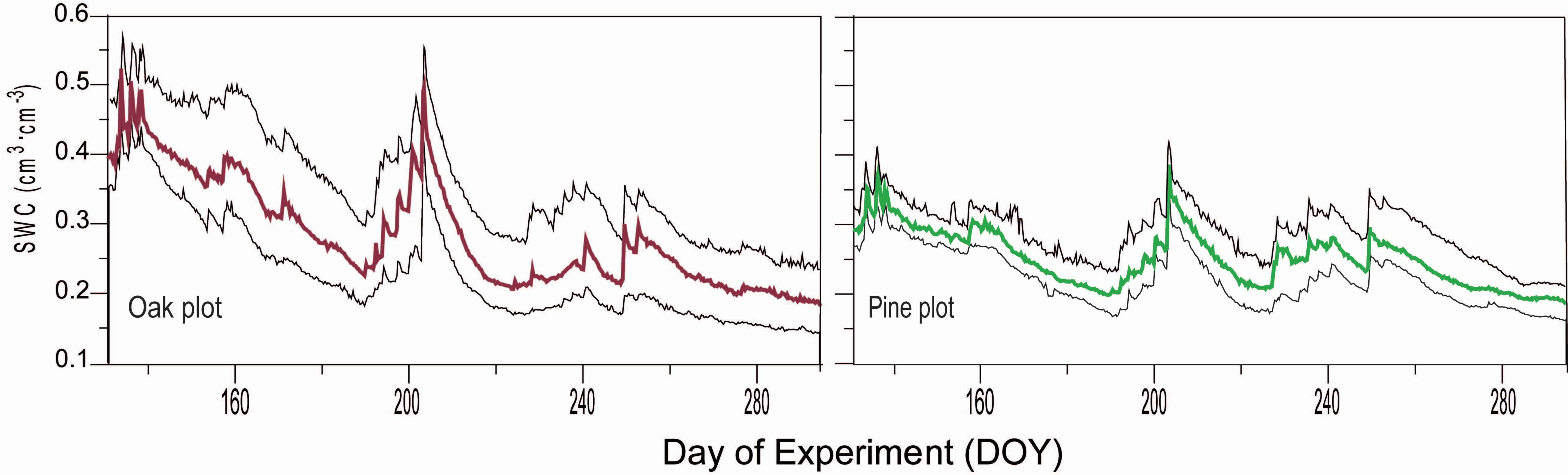

0.6
0.5
0.4
0.3
0.2
0.1
SWC (cm^3·cm^-3)
Oak plot
Pine plot
160
200
240
280
Day of Experiment (DOY)

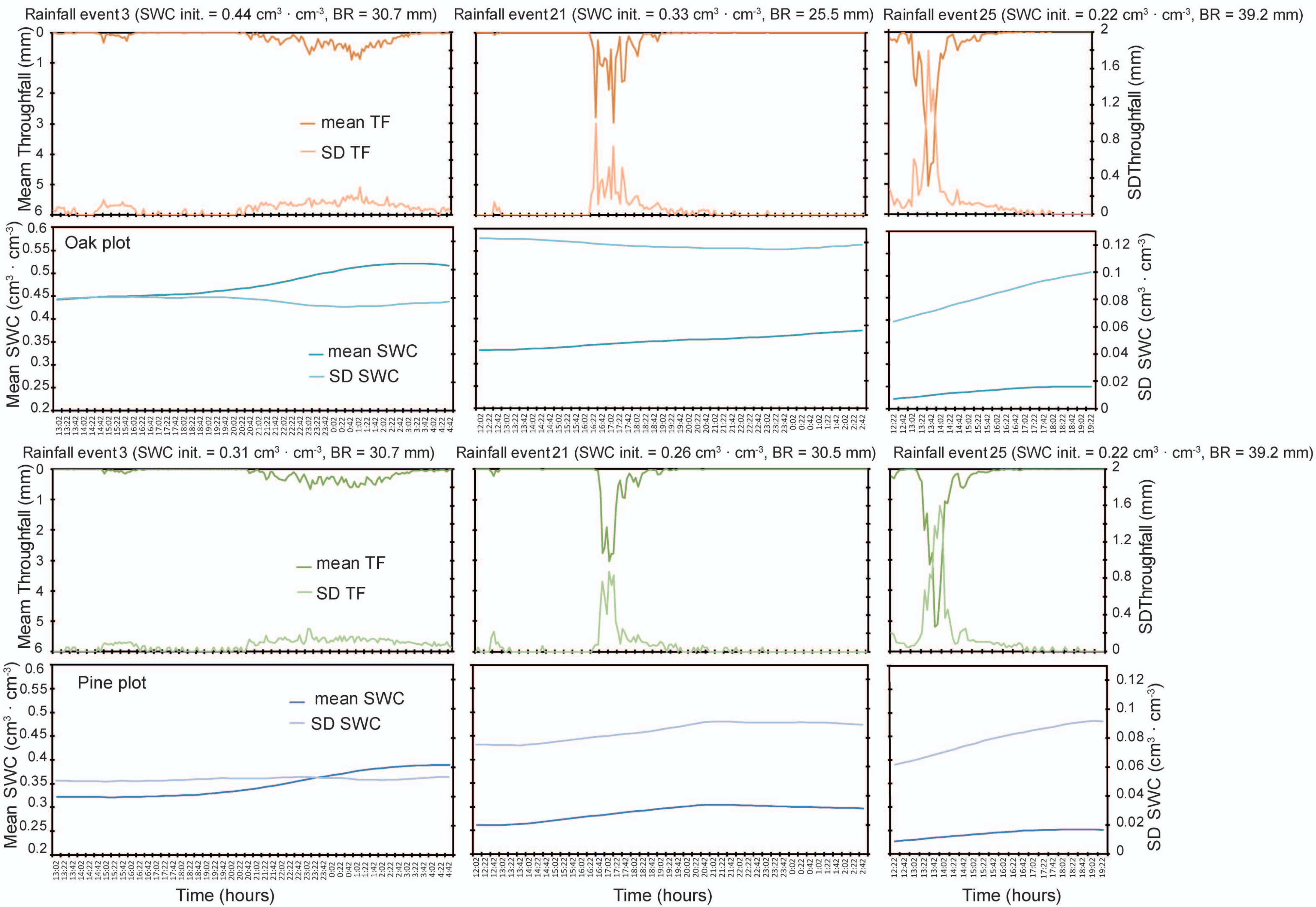

Rainfall event 3 (SWC init. = 0.44 cm³ · cm⁻³, BR = 30.7 mm)
Rainfall event 21 (SWC init. = 0.33 cm³ · cm⁻³, BR = 25.5 mm)
Rainfall event 25 (SWC init. = 0.22 cm³ · cm⁻³, BR = 39.2 mm)
Meam Throughfall (mm)
SDThroughfall (mm)
mean TF
SD TF
Oak plot
Mean SWC (cm³ · cm⁻³)
SD SWC (cm³ · cm⁻³)
mean SWC
SD SWC
Rainfall event 3 (SWC init. = 0.31 cm³ · cm⁻³, BR = 30.7 mm)
Rainfall event 21 (SWC init. = 0.26 cm³ · cm⁻³, BR = 30.5 mm)
Rainfall event 25 (SWC init. = 0.22 cm³ · cm⁻³, BR = 39.2 mm)
Meam Throughfall (mm)
SDThroughfall (mm)
mean TF
SD TF
Pine plot
mean SWC
SD SWC
Mean SWC (cm³ · cm⁻³)
SD SWC (cm³ · cm⁻³)
Time (hours)
Time (hours)
Time (hours)

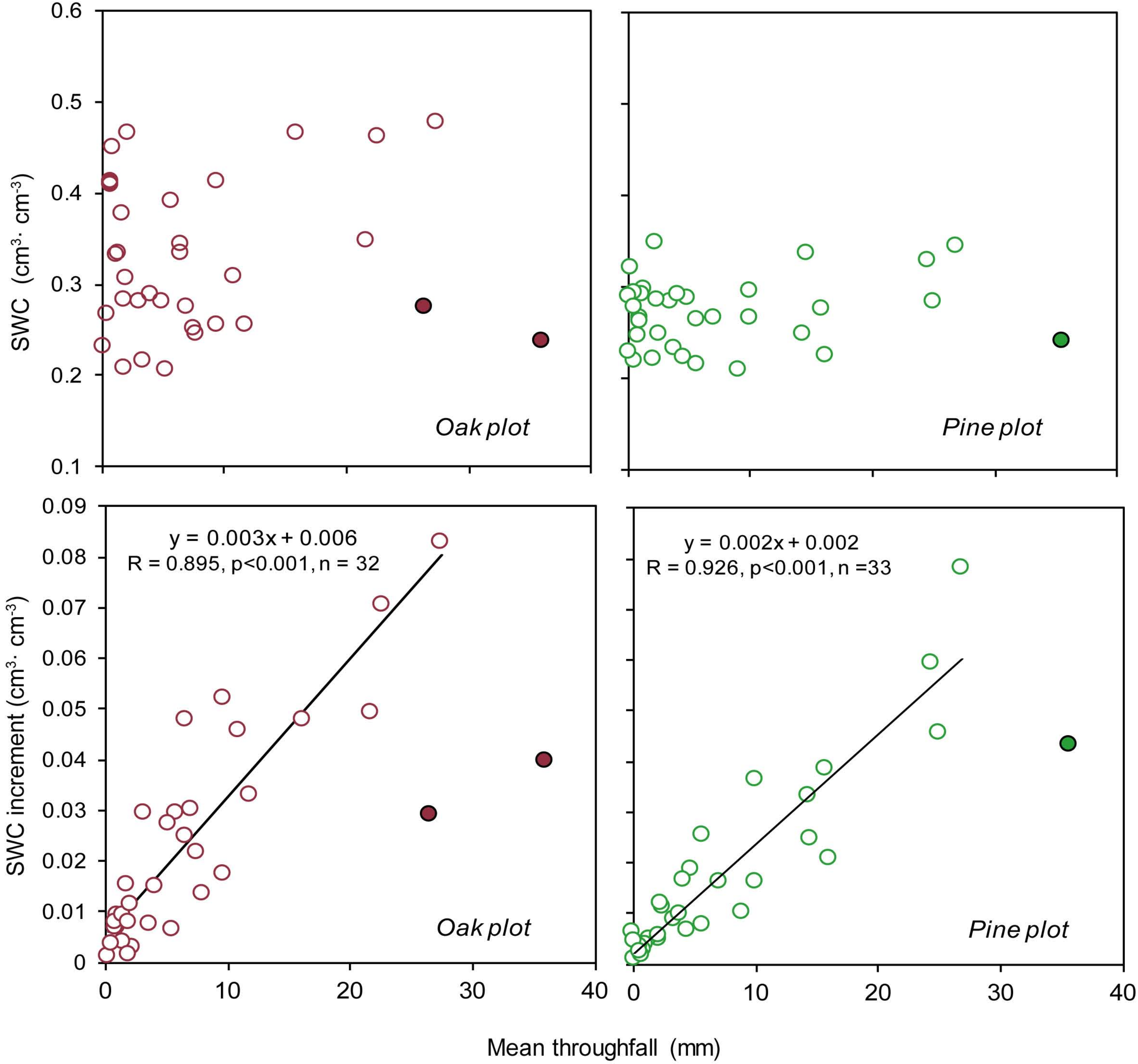
0.6
0.5
0.4
0.3
0.2
0.1
SWC (cm³· cm⁻³)
Oak plot
Pine plot
0.09
0.08
0.07
0.06
0.05
0.04
0.03
0.02
0.01
0
SWC increment (cm³· cm⁻³)
y = 0.003x + 0.006
R = 0.895, p<0.001, n = 32
y = 0.002x + 0.002
R = 0.926, p<0.001, n =33
Oak plot
Pine plot
0
10
20
30
40
Mean throughfall (mm)

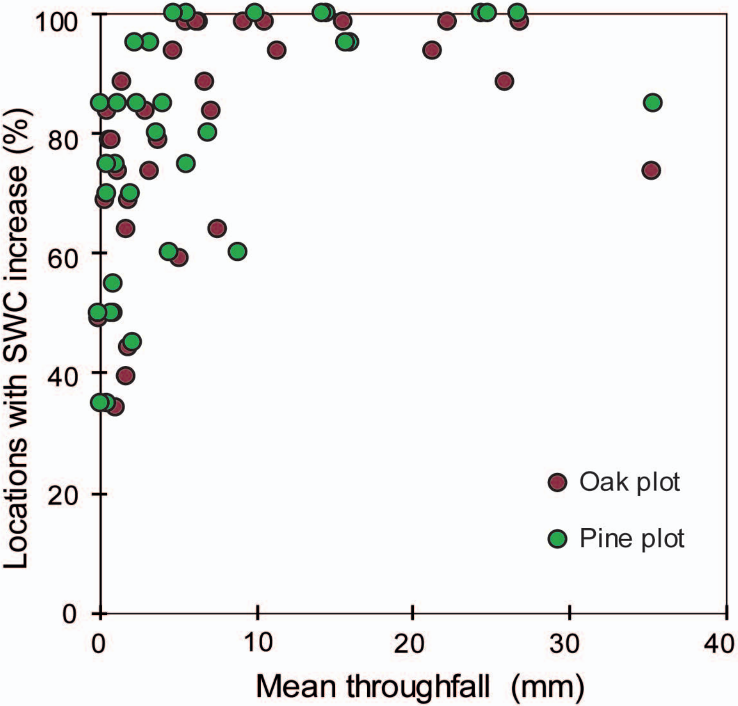

Locations with SWC increase (%)
100
80
60
40
20
0
0
10
20
30
40
Mean throughfall (mm)
Oak plot
Pine plot

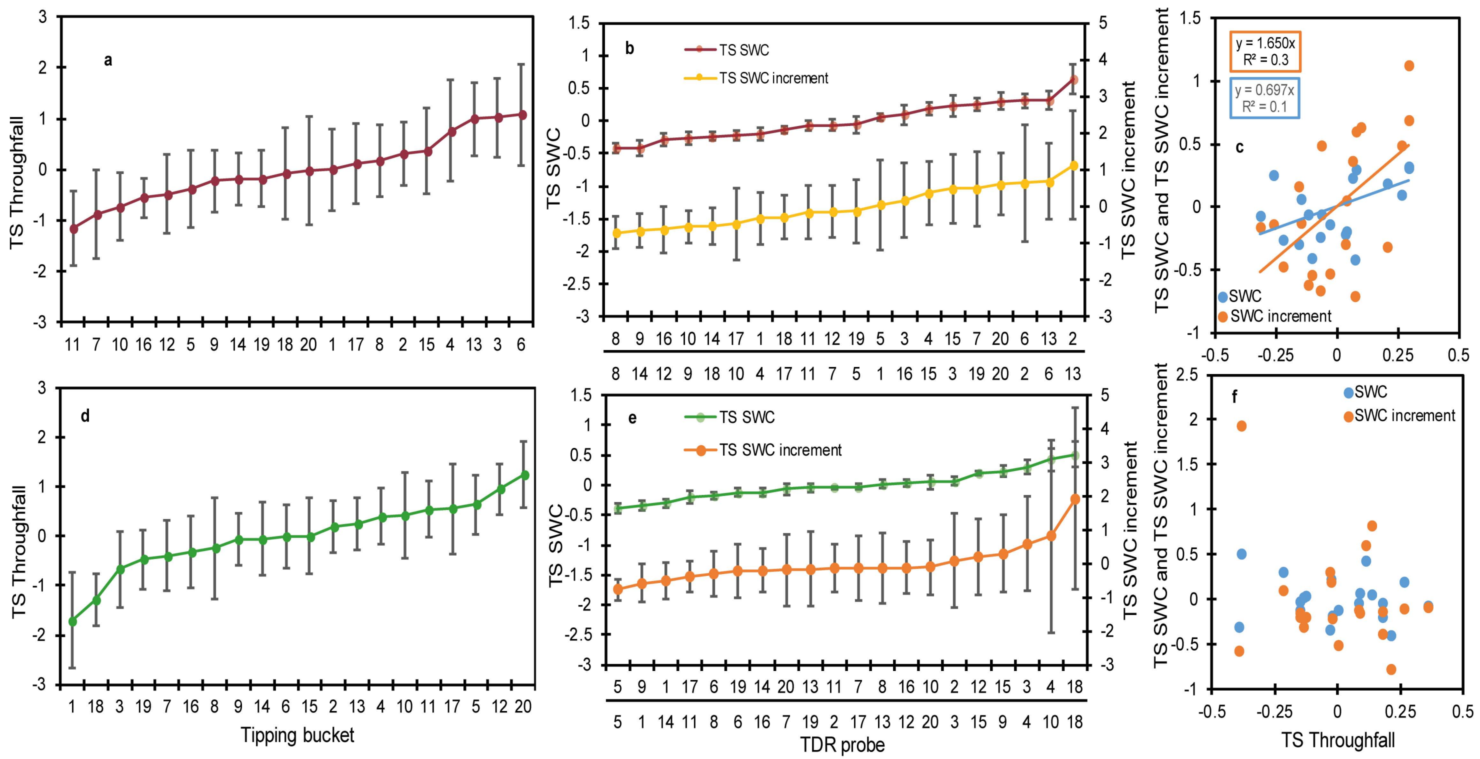

a
b
TS SWC
TS SWC increment
c
y = 1.650x
R² = 0.3
y = 0.697x
R² = 0.1
SWC
SWC increment
d
e
f
TS Throughfall
TS SWC
TS SWC increment
TS SWC and TS SWC increment
Tipping bucket
TDR probe

Appendix A: Rainfall characteristics and meteorological conditions during the rainfall events considered in this study for the both forest plots. I: mean intensity, I_0: maximum intensity in 5 minutes; D: duration, M: magnitude; The rainfall events are grouped by mean intensity (VL: very light, L: light, M: moderate, H: heavy, VH: very heavy, E: extreme) following Garcia-Estringana et al. (2011), by duration (long or short) following Llasat et al. (2001) and by amount (large or small) following Garcia-Estringana et al. (2011). T: mean air temperature; RH: mean air relative humidity; Rn: mean net radiation; Rn cum.: cumulated net radiation; WS: wind speed and WD: wind direction.

					Rainfall characteristics				Meteorological characteristics during the rainfall event					
Oak plot	M	D	I	I_0		Classes			T	RH	Rn	Rn cum.	WS	WD
Event	(mm)	(h)	(mm h^{-1})	(mm h^{-1})	Start date, time	I	D	M	(ºC)	(%)	(Wm2)	MJ m^{-2}	(m/s)	(º)
1	25.8	13.0	2.0	12.6	15/05,11:05	L	Long	Large	7.6	100.7	12.7	0.6	0.8	99.6
2	1.4	1.5	0.9	7.0	16/05, 15:00	VL	Short	Small	7.4	75.1	42.6	0.2	1.9	220.4
3	30.7	17.2	1.8	11.1	17/05, 12:50	L	Long	Large	4.2	96.5	3.1	0.2	0.4	224.8
4	2.6	1.2	2.0	5.6	18/05, 16:25	M	Short	Small	5.6	89.8	11.9	0.1	0.5	223.3
5	19.3	37.5	0.5	6.9	19/05, 09:05	VL	Long	Large	6.0	88.1	-12.4	-0.1	2.9	154.4
6	1.8	2.3	0.8	2.7	28/05, 11:05	VL	Short	Small	9.9	80.6	202.5	1.6	2.5	
7	1.6	2.4	0.6	7.0	29/05, 10:30	VL	Short	Small	7.6	67.4	278.3	2.5	1.5	95.7
8	8.0	4.4	1.8	23.7	04/06, 13:10	L	Short	Small	14.1	72.4	45.7	0.7	1.5	
9	12.6	3.7	3.4	39.2	08/06, 05:50	M	Short	Large	9.0	92.0	4.3	0.1	1.2	188.3
10	2.0	1.9	1.0	2.8	09/06, 11:05	L	Short	Small	11.3	87.3	98.6	0.7	0.3	324.0
11	3.1	9.8	0.3	5.6	17/06, 19:35	VL	Short	Small	15.2	92.8	-32.3	-0.6	0.9	158.9
12	2.7	4.6	0.6	2.8	18/06, 18:30	VL	Short	Small	15.2	92.8	-22.4	-0.4	0.9	126.3
13	7.4	2.6	2.8	24.0	21/06, 17:55	M	Short	Large	12.5	94.6	-29.3	-0.3	1.0	81.2
14	4.1	2.3	1.8	5.6	01/07, 16:10	L	Short	Small	15.4	75.9	-104.0	-0.9	2.3	270.1
15	11.2	8.2	1.4	12.6	10/07, 12:25	L	Short	Large	17.1	88.8	21.0	0.6	1.2	212.7

16	28.6	1.0	25.5	114.6	12/07, 18:55	E	Short	Large	13.6	94.0	-48.5	-0.2	2.8	190.0
17	6.8	4.8	1.4	25.2	13/07, 14:55	L	Short	Small	17.2	73.3	-49.9	-0.9	1.0	219.0
18	13.2	8.2	1.6	44.8	14/07, 11:35	L	Short	Large	17.3	80.2	41.4	1.2	1.4	196.3
19	2.9	0.7	4.3	8.0	16/07, 19:25	M	Short	Small	19.3	70.9	-65.0	-0.2	0.4	139.8
20	8.5	9.5	0.9	8.0	17/07, 19:10	VL	Short	Small	14.5	97.4	-33.8	-1.2	0.8	256.0
21	25.5	8.7	2.9	40.0	20/07, 12:45	M	Short	Large	17.4	82.1	61.1	1.9	0.9	126.3
22	3.8	10.8	0.3	13.3	20/07, 11:55	VL	Long	Small	20.4	66.7	37.3	1.5	1.3	68.3
23	1.2	1.6	0.7	6.9	07/08, 23:45	VL	Short	Small	14.9	61.5	-99.4	-0.6	3.8	285.1
24	4.5	3.9	1.1	16.0	13/08, 13:30	L	Short	Small	17.5	90.2	-6.3	-0.1	0.8	135.1
25	39.2	3.9	10.0	62.7	16/08, 12:10	VH	Short	Large	16.8	93.7	-32.8	-0.5	1.2	191.6
26	10.7	0.7	16.0	51.4	17/08, 14:50	VH	Short	Large	16.8	87.0	-75.6	-0.2	2.6	140.9
27	8.7	0.6	14.8	55.9	22/08, 17:00	VH	Short	Large	21.2	65.2	-110.0	-0.3	2.4	225.4
28	12.9	6.2	2.1	45.9	24/08, 12:40	M	Short	Large			68.4	1.5	1.5	141.3
29	8.8	2.4	3.6	12.5	26/08, 19:40	M	Short	Small			-7.2	-0.1	0.3	91.6
30	6.6	1.0	6.6	27.8	29/08, 17:55	H	Short	Small			-33.0	-0.1	1.0	182.7
31	5.6	9.3	0.6	5.6	10/09, 10:50	VH	Short	Small			107.6	3.6	0.1	64.9
32	1.2	0.3	3.5	5.6	15/09, 03:35	M	Short	Small			-14.9	0.0	0.4	135.0
33	7.2	2.4	3.0	32.1	04/10, 15:35	M	Short	Small			-47.4	-0.4	1.5	157.1
34	3.1	3.2	1.0	5.6	05/10, 17:10	VL	Short	Small			-25.4	-0.3	0.7	141.8

					Rainfall characteristics				Meteorological characteristics during the rainfall event					
Pine plot	M	D	I	I_0		Classes			T	RH	Rn	Rn cum.	WS	WD
Event	(mm)	(h)	(mm h^{-1})	(mm h^{-1})	Start date, time	I	D	M	(ºC)	(%)	(Wm^2)	MJ m^{-2}	(m/s)	(º)
1	29.4	11.7	2.5	12.8	15/05, 10:05	M	Long	Large	6.8	96.9	25.8	1.1	0.8	158.0
2	1.3	3.0	0.4	2.6	16/05, 13:25	VL	Short	Small	6.9	77.1	205.8	2.3	1.5	200.3
3	30.7	22.7	1.4	7.7	17/05, 12:50	L	Long	Large	3.8	89.6	105.4	8.6	1.1	189.0
4	3.4	1.8	1.9	7.7	18/05, 15:45	L	Short	Small	5.0	84.6	39.2	0.3	1.0	181.0
5	19.4	28.4	0.7	7.7	19/05, 09:05	VL	Long	Large	4.2	92.9	58.1	6.0	0.6	185.5
6	3.8	2.5	1.5	5.1	28/05, 10:50	L	Short	Small	8.9	80.4	199.5	4.6	1.6	184.7
7	3.0	6.2	0.5	5.1	29/05, 12:35	VL	Short	Small	9.4	73.0	202.5	4.6	1.7	213.5
8	6.0	1.2	5.2	18.2	04/06, 16:25	H	Short	Small	10.4	85.9		109.7	1.8	205.1
9	13.2	3.6	3.7	33.3	08/06, 05:45	M	Short	Large	8.0	87.9	-0.1	0.0	1.3	187.7
10	1.7	3.5	0.5	2.6	09/06, 10:55	VL	Short	Small	10.2	85.3	148.0	1.9	0.8	124.0
11	3.2	9.7	0.3	7.7	17/06, 19:30	VL	Short	Small	15.3	80.8	9.4	0.3	1.0	213.2
12	2.1	1.8	1.2	2.6	18/06, 21:10	L	Short	Small	13.7	96.1	-10.3	-0.1	0.5	140.0
13	2.1	3.3	0.7	7.7	21/06, 17:40	VL	Short	Small	11.8	88.4	-28.0	-0.3	1.2	244.1
14	2.6	2.1	1.2	5.1	01/07, 16:20	L	Short	Small	14.2	71.8	-86.3	-0.7	2.5	279.5
15	13.2	7.9	1.7	15.4	10/07, 12:25	L	Short	Large	16.0	85.4	33.9	1.0	1.2	191.2
16	19.2	1.0	19.2	89.6	12/07, 19:10	VH	Short	Large	13.3	89.4	-24.0	-0.1	2.4	200.8
17	8.3	4.8	1.7	23.0	13/07, 14:50	L	Short	Small	17.8	66.2	86.2	1.5	1.8	235.0
18	18.1	6.3	2.9	48.6	14/07, 14:05	M	Short	Large	14.2	82.4	-25.1	-0.6	1.4	208.9
19	4.1	0.7	6.1	15.4	16/07, 19:20	H	Short	Small	15.3	85.3	-41.7	-0.1	1.2	256.0
20	9.0	9.5	0.9	7.7	17/07, 18:55	VL	Short	Small	13.7	91.1	-29.3	-1.0	1.1	206.1
21	30.5	7.9	3.9	41.0	20/07, 12:05	M	Short	Large	16.9	76.9	40.6	1.0	1.5	197.4
22	1.3	7.2	0.2	2.6	21/07, 11:55	VL	Short	Small	21.1	63.4	136.2	3.6	1.5	152.4
23	1.3	0.2	7.7	10.2	08/08, 01:00	H	Short	Small	13.3	66.1	-128.0	-0.1	2.3	185.0
24	9.2	4.1	2.2	25.6	13/08, 13:25	M	Short	Small	16.4	83.9	-23.1	-0.3	1.2	224.9
25	39.2	3.8	10.5	74.3	16/08, 12:20	VH	Short	Large	15.6	89.5	-34.2	-0.5	1.7	206.1
26	13.0	0.6	22.3	61.5	17/08, 14:50	E	Short	Large	15.7	85.1	-61.1	-0.1	1.8	128.0
27	9.0	0.8	10.8	58.9	22/08, 17:00	VH	Short	Small	16.6	80.6	-63.1	-0.2	2.5	240.0

28	18.6	6.0	3.1	51.2	24/08, 13:35	M	Short	Large	17.9	80.0	42.6	0.9	1.1	197.4
29	7.3	2.2	3.3	10.2	26/08, 19:20	M	Short	Small	11.9	94.5	-6.9	-0.1	0.4	214.1
30	6.4	1.2	5.5	23.0	29/08, 17:50	M	Short	Small	12.7	87.8	-28.5	-0.1	1.3	221.6
31	5.3	9.5	0.6	7.7	10/09, 10:40	VL	Short	Small	14.1	85.7	99.4	3.4	0.6	165.8
32	1.7	0.3	6.8	5.1	15/09, 03:35	H	Short	Small	13.1	95.3	-4.9	0.0	0.6	191.0
33	6.8	2.3	3.0	38.4	04/10, 15:35	M	Short	Small	13.4	85.0	-32.9	-0.3	1.5	239.0
34	3.6	5.2	0.7	7.7	05/10, 14:10	VL	Short	Small	12.4	91.3	-5.1	-0.1	0.8	205.8

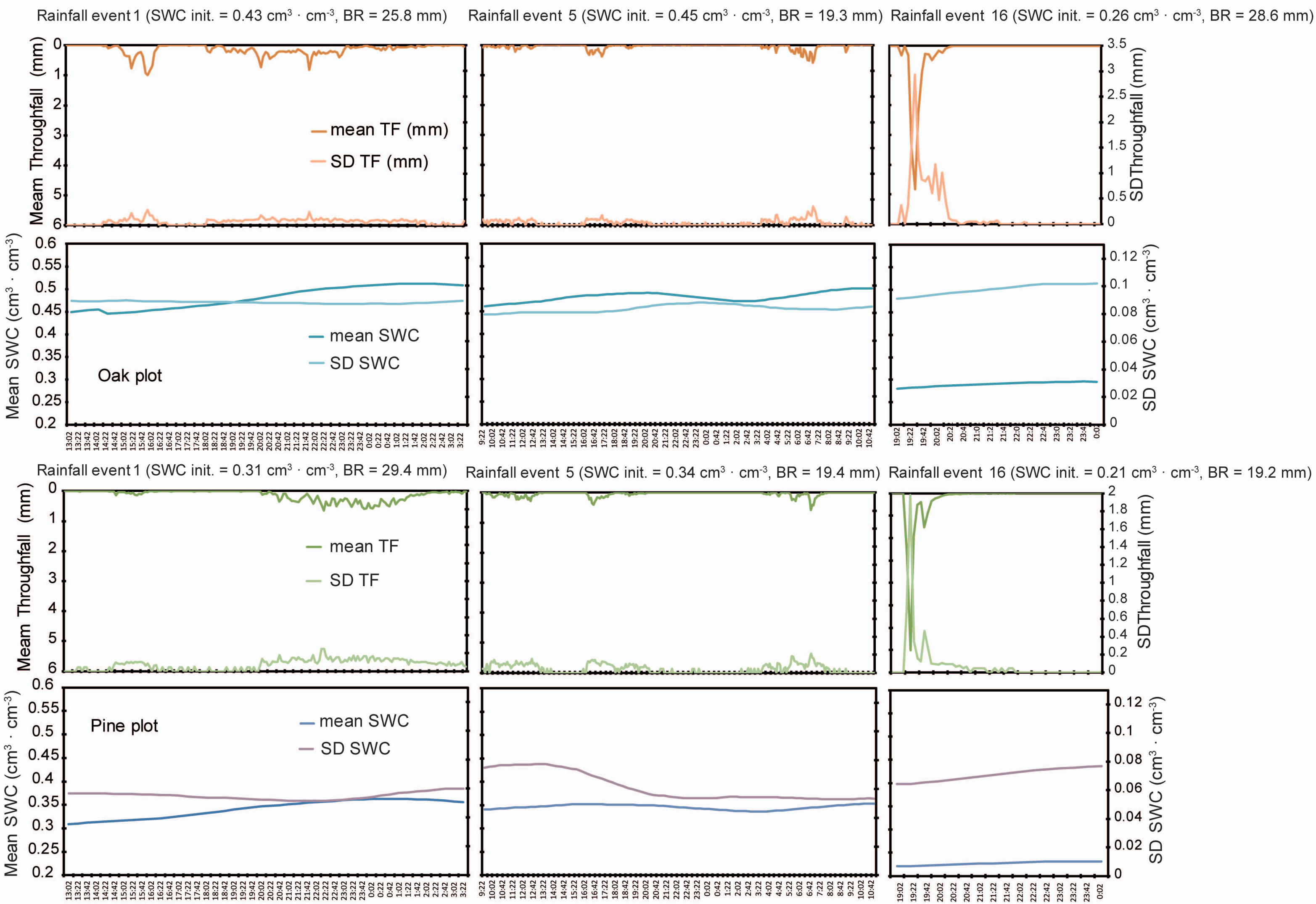

Rainfall event 1 (SWC init. = 0.43 cm³ · cm⁻³, BR = 25.8 mm)
Rainfall event 5 (SWC init. = 0.45 cm³ · cm⁻³, BR = 19.3 mm)
Rainfall event 16 (SWC init. = 0.26 cm³ · cm⁻³, BR = 28.6 mm)
Meam Throughfall (mm)
SDThroughfall (mm)
mean TF (mm)
SD TF (mm)
Mean SWC (cm³ · cm⁻³)
SD SWC (cm³ · cm⁻³)
mean SWC
SD SWC
Oak plot
Rainfall event 1 (SWC init. = 0.31 cm³ · cm⁻³, BR = 29.4 mm)
Rainfall event 5 (SWC init. = 0.34 cm³ · cm⁻³, BR = 19.4 mm)
Rainfall event 16 (SWC init. = 0.21 cm³ · cm⁻³, BR = 19.2 mm)
Meam Throughfall (mm)
SDThroughfall (mm)
mean TF
SD TF
Pine plot
mean SWC
SD SWC
Mean SWC (cm³ · cm⁻³)
SD SWC (cm³ · cm⁻³)

Appendix C. Pearson correlations between the dependent (SWC increase, cm^3/cm^3) and independent variables studied for the oak and the pine plots: TF: throughfall amount (mm), TF max int.: throughfall maximum intensity (mm/h), TF mean int.: throughfall mean intensity (mm/h), DBH: diameter at breast height of the nearest tree (cm), D: distance to the nearest tree (m), FC: forest cover above location (%), H: height of the nearest tree (m), V: crown volume of the nearest tree (m^3), ps: soil bulk density (g/cm^3), Ao: forest floor thickness (cm), SOC: soil organic carbon (%), SWC init.: antecedent soil water content (cm^3/cm^{-3}). ** significant at p-level<0.01, * significant at p-level<0.05.

Oak plot	***SWC increase***	***TF***	***TF max int.***	***TF mean int.***	***DBH***	***D***	***FC***	***H***	***V***	***ps***	***Ao***	***SOC***	***SWC init.***
SWC increase	1	.513**	.156**	0.049	-0.030	0.068	-.117**	.099**	-.076*	0.103	-.268**	.212**	.265**
TF	.513**	1	.637**	.484**	0.014	0.037	-0.026	0.011	-0.008	0.015	-0.046	0.059	0.026
TF max int.	.156**	.637**	1	.878**	0.018	0.020	-0.018	0.009	0.008	0.010	-0.042	0.035	-.207**
TF mean int.	0.049	.484**	.878**	1	0.014	0.029	-0.019	0.012	-0.001	0.016	-0.033	0.042	-.191**
DBH	-0.030	0.014	0.018	0.014	1	0.382	0.021	0.154	.748**	0.200	0.118	0.535	-.145**
D	0.068	0.037	0.020	0.029	0.382	1	-.599**	0.246	0.275	-0.035	-0.103	0.556	0.049
FC	-.117**	-0.026	-0.018	-0.019	0.021	-.599**	1	-0.152	-0.021	-0.142	0.205	-0.497	-.200**
H	.099**	0.011	0.009	0.012	0.154	0.246	-0.152	1	0.108	-0.158	-0.459	-0.288	-0.047
V	-.076*	-0.008	0.008	-0.001	.748**	0.275	-0.021	0.108	1	0.540	0.042	0.003	-.244**
ps	0.103	0.015	0.010	0.016	0.200	-0.035	-0.142	-0.158	0.540	1	-0.064	0.073	-0.070
Ao	-.268**	-0.046	-0.042	-0.033	0.118	-0.103	0.205	-0.459	0.042	-0.064	1	-0.368	-.519**
SOC	.212**	0.059	0.035	0.042	0.535	0.556	-0.497	-0.288	0.003	0.073	-0.368	1	.354**
SWC init.	.265**	0.026	-.207**	-.191**	-.145**	0.049	-.200**	-0.047	-.244**	-0.070	-.519**	.354**	1

Pine plot	***SWC increase***	***TF***	***TF max int.***	***TF mean int.***	***DBH***	***D***	***FC***	***H***	***V***	***ps***	***Ao***	***SOC***	***SWC init.***
SWC increase	1	.613**	.091*	.093*	0.015	-.113**	.090*	.085*	0.002	.209**	-.214**	0.032	.177**
TF	.613**	1	.145**	.077*	0.005	0.003	-0.004	0.007	0.023	0.063	-0.055	-0.061	-0.038
TF max int.	.091*	.145**	1	.655**	0.016	-0.026	0.009	0.028	0.022	0.067	-0.053	-0.041	-0.072
TF mean int.	.093*	.077*	.655**	1	0.009	-0.004	-0.003	0.014	0.016	0.052	-0.040	-0.046	-0.068
DBH	0.015	0.005	0.016	0.009	1	0.181	0.417	.602**	.847**	0.384	0.095	0.413	-0.037
D	-.113**	0.003	-0.026	-0.004	0.181	1	-0.262	0.010	0.159	-0.637	0.641	-0.057	-.083*
FC	.090*	-0.004	0.009	-0.003	0.417	-0.262	1	0.186	.485*	.735*	-0.478	-0.001	.100**
H	.085*	0.007	0.028	0.014	.602**	0.010	0.186	1	0.374	0.060	0.141	0.057	0.064
V	0.002	0.023	0.022	0.016	.847**	0.159	.485*	0.374	1	0.579	-0.168	0.158	-0.043
ps	.209**	0.063	0.067	0.052	0.384	-0.637	.735*	0.060	0.579	1	-.794*	-0.148	.559**
Ao	-.214**	-0.055	-0.053	-0.040	0.095	0.641	-0.478	0.141	-0.168	-.794*	1	0.163	-.620**
SOC	0.032	-0.061	-0.041	-0.046	0.413	-0.057	-0.001	0.057	0.158	-0.148	0.163	1	-0.012
SWC init.	.177**	-0.038	-0.072	-0.068	-0.037	-.083*	.100**	0.064	-0.043	.559**	-.620**	-0.012	1

Appendix D. Some model structures tested in the GMLMs for the two sites. Marginal R^2 represents the proportion of deviance explained by the fixed predictors; Conditional R^2 represents the proportion of deviance explained by the fixed and random (location and rainfall event) predictors; ΔAIC is the change in the Akaike (AIC) value respect to the one giving the most negative AIC as the most optimal model. Fixed predictors: TF: throughfall amount (mm), FC: forest cover above location (%), V: crown volume of the nearest tree (m^3), ps: soil bulk density (g/cm^3), Ao: litter thickness (cm), SOC: soil organic carbon (%).

Oak plot	Model	Marginal R^2	Conditional R^2	ΔAIC	Model structure (fixed predictors)
	CB1	0.38	0.93	3.88	ps+Ao+SOC+TF+V+FC
	CB2	0.38	0.93	1.98	ps+Ao+SOC+TF+V
	CB3	0.38	0.93	3.07	ps+Ao+SOC+TF+FC
	CB4	0.36	0.93	4.96	Ao+SOC+TF+FC
	CB5	0.38	0.93	3.12	ps+Ao+TF+FC
	CB6	0.34	0.93	7.54	ps+SOC+TF+V+FC
	CB7	0.38	0.93	1.15	ps+Ao+SOC+TF
	CB8	0.38	0.93	0.23	ps+Ao+TF
	CB9	0.38	0.93	0.98	Ao+SOC+TF
	CB10	0.37	0.93	0.56	Ao+TF

Pine plot	Model	Marginal R^2	Conditional R^2	ΔAIC	Model structure (fixed predictors)
	CR1	0.44	0.95	4.07	ps+Ao+SOC+TF+V+FC
	CR2	0.45	0.94	3.17	ps+Ao+SOC+TF+V
	CR3	0.43	0.94	4.93	ps+Ao+SOC+TF+FC
	CR4	0.45	0.94	3.11	Ao+SOC+TF+V+FC
	CR5	0.45	0.94	3.76	ps+Ao+TF+V+FC
	CR6	0.46	0.94	2.11	ps+SOC+TF+V+FC
	CR7	0.45	0.94	3.20	ps+Ao+SOC+TF
	CR8	0.45	0.94	1.84	ps+Ao+TF
	CR9	0.46	0.94	0.26	ps+TF
	CR10	0.46	0.94	1.39	Ao+SOC+TF
	CR11	0.46	0.94	0.00	Ao+TF